

**Therapeutic concentrations of antidepressants inhibit  
pancreatic beta-cell function via mitochondrial complex  
inhibition**

Journal:	<i>Toxicological Sciences</i>
Manuscript ID	TOXSCI-17-0009.R2
Manuscript Type:	Research Article
Date Submitted by the Author:	n/a
Complete List of Authors:	Elmorsy, Ekramy; Mansoura University Faculty of Medicine, Forensic Medicine and Clinical Toxicology Al-Ghafari, Ayat; King Abdulaziz University, Biochemistry Helaly, Ahmed; Mansoura University Faculty of Medicine, Forensic Medicine and Clinical Toxicology Hisab, Ahmed; University of Nottingham, Life Sciences Oehrle, Bettina; University of Nottingham, Life Sciences Smith, Paul; University of Nottingham,
Key Words:	Antidepressant, Diabetes mellitus, beta-cell, mitochondria, cytotoxicity < In Vitro and Alternatives, fluoxetine

**Therapeutic concentrations of antidepressants inhibit pancreatic beta-cell function via mitochondrial complex inhibition**

**Ekramy Elmorsy\* Ayat Al-Ghafari† Ahmed N.M. Helaly\* Ahmed S. Hisab‡ Bettina Oehrle‡ Paul A. Smith‡¶**

**Affiliations**

\*Department of Forensic Medicine and Clinical Toxicology, Faculty of Medicine, Mansoura University, Egypt.

†Biochemistry Department, Faculty of Science, King Abdulaziz University (KAU), Jeddah, Kingdom of Saudi Arabia

‡University of Nottingham Medical School, University of Nottingham, UK, NG9 4BD

**¶ Corresponding Author**

Email: [Paul.a.smith@nottingham.ac.uk](mailto:Paul.a.smith@nottingham.ac.uk)

Tel+ 44 (0)115 849 3227

Fax +44 (0)115 823 0142

**Running title:** Antidepressant toxicity on beta-cells

## Abstract

Diabetes mellitus risk is increased by prolonged usage of antidepressants (ADs). Although various mechanisms are suggested for their diabetogenic potential, whether a direct effect of ADs on pancreatic  $\beta$ -cells is involved is unclear. We examined this idea for three ADs: paroxetine, clomipramine and, with particular emphasis, fluoxetine, on insulin secretion, mitochondrial function, cellular bioenergetics, KATP channel activity and caspase activity in murine and human cell-line models of pancreatic  $\beta$ -cells. Metabolic assays showed that these ADs decreased the redox, oxidative respiration and energetic potential of  $\beta$ -cells in a time and concentration dependent manner, even at a concentration of 100 nM, well within the therapeutic window. These effects were related to inhibition of mitochondrial complex I and III. Consistent with impaired mitochondrial function, lactate output was increased and insulin secretion decreased. Neither fluoxetine, antimycin nor rotenone could reactivate KATP channel activity blocked by glucose unlike the mitochondrial uncoupler, FCCP. Chronic, but not acute, AD increased oxidative stress and activated caspases, 3, 8 and 9. A close agreement was found for the rates of oxidative respiration, lactate output and modulation of KATP channel activity in MIN6 cells with those of primary murine cells; data that supports MIN6 as a valid model to study beta-cell bioenergetics. To conclude, paroxetine, clomipramine and fluoxetine were all cytotoxic at therapeutic concentrations on pancreatic beta-cells; an action suggested to arise by inhibition of mitochondrial bioenergetics, oxidative stress and induction of apoptosis. These actions help explain the diabetogenic potential of these ADs in humans.

**Keywords:** Antidepressant, Diabetes mellitus, beta-cell, mitochondria, cytotoxicity, fluoxetine.

## Introduction

Antidepressants (ADs) play a key role in treating depression as well as other psychiatric disorders including anxiety and obsessive-compulsive disorders. However, clinical studies indicate that the tricyclic antidepressant (TCA) and serotonin selective reuptake inhibitor (SSRI) classes of AD are particularly associated with increased risks of hyperglycaemia and type 2 diabetes mellitus (T2D) (Lustman et al., 1997; Rubin et al., 2008; Brown et al., 2008; Derijks et al., 2008; Andersohn et al., 2009; Kivimäki et al., 2010; Khoza et al., 2011). Although weight gain is a common side effect of AD usage (Uguz et al., 2015) and a risk factor for T2D (Andersohn et al., 2009; Kivimäki et al., 2010;), when weight is controlled for, ADs still increase T2D risk (Rubin et al., 2008; Pan et al., 2012).

The effects of ADs on glucose homeostasis have been widely studied *in-vivo* in rodents. The SSRI fluoxetine when administered acutely produces hyperglycaemia without hyperinsulinaemia (Yamada et al., 1999; Gomez et al., 2001), actions suggestive of a direct inhibition of insulin secretion. Similar trends are observed with clomipramine, a TCA, which also produces acute hyperglycaemia without hyperinsulinaemia in rodents (Sugimoto et al., 2003; Gomez et al., 2001) as well as in humans (Lustman et al., 1997; McIntyre et al., 2006). In murine models, intraperitoneal administration of fluoxetine or clomipramine produces maximal hyperglycaemia within the first 30-90 minutes of injection (Yamada et al., 1999; Sugimoto et al., 2003; Gomez et al., 2001); observations that also indicate a direct action of these drugs on the  $\beta$ -cell, an idea further supported by their ability to inhibit insulin secretion from isolated pancreatic  $\beta$ -cells (Antoine et al., 2004; Cataldo et al., 2015).

The mechanism of glucose stimulus-secretion coupling of insulin from the pancreatic  $\beta$ -cell is well understood, with an essential role played by oxidative metabolism of the sugar (Ashcroft et al., 1994; Maechler 2002). Clearly, any compound that interferes with mitochondrial bioenergetics and oxidative metabolism will impair insulin secretion; for example the mitochondrial Complex I inhibitor rotenone (MacDonald & Fahien, 1990; Zhou et al., 1999), Complex III inhibitor antimycin (Meglasson et al., 1987; MacDonald & Fahien, 1990),  $F_0F_1$ ATPase inhibitor oligomycin (Zhou et al., 1999; Ortsäter et al., 2002) and protonophore uncoupler FCCP (MacDonald & Fahien, 1990; Ortsäter et al., 2002) all act to achieve this.

The ADs, amitriptyline, amoxapine, citalopram, clomipramine and fluoxetine all cause mitochondrial dysfunction in other cell systems (Weinbach et al., 1986; Eto et al., 1985; Souza et

al., 1994; Xia et al., 1999; Curti et al., 1999; Chan et al., 2005). Where such events can culminate in oxidative stress and induction of apoptosis (Abdel-Razaq et al., 2011; Li et al., 2012), whether the same is true of pancreatic beta-cells is unknown

Mitochondria have key roles in the function of many other cell types, in particular those with a high energetic demand, for example sensory cells, neurons, skeletal and cardiac muscle. Why reports of adverse effects of chronic AD usage only appear for pancreatic  $\beta$ -cell function and not that of other tissue suggests that the mitochondria of the  $\beta$ -cell may be unique in its sensitivity to these classes of drugs. Indeed the predicted side effects of mitochondrial dysfunction in other cell types, whose function depends heavily on this organelle function: impaired vision, hearing loss, cardiac failure and skeletal muscle weakness, are not normally associated with AD usage (Joint Formulary Committee., 2016).

Although mitochondria have key roles in many cell types, whether the diabetogenic effect of ADs is indeed mediated by action of these drugs on this organelle in pancreatic beta-cells has not been explored. In this study, the ability of three ADs: paroxetine, fluoxetine and clomipramine, with particular emphasis on fluoxetine, to disrupt mitochondrial function, impair bioenergetics and inhibit insulin secretion of native and cell-line models of murine pancreatic  $\beta$ -cells was investigated. We investigated the metabolic actions of ADs over a concentration range that encompassed both therapeutic (fluoxetine  $\sim 0.4$  to  $1.6 \mu\text{M}$ , paroxetine  $\sim 0.03$  to  $0.4 \mu\text{M}$ , clomipramine  $\sim 0.3$  to  $1.3 \mu\text{M}$ ) as well as toxic plasma levels (fluoxetine  $> 3 \mu\text{M}$ , paroxetine  $> 1 \mu\text{M}$ , clomipramine  $> 1.3 \mu\text{M}$ ; Reis et al., 2009; Winek et al., 2001; Schulz et al., 2012). In addition we explored both the effect of chronic actions of these drugs in order to mimic their long term usage, as well as their acute actions at higher concentrations in an attempt to mimic overdose and drug-drug interaction situations. Lastly, we have also explored the relationship between mitochondrial blockade and modulation of the ATP-sensitive  $\text{K}^+$  channels, a key signaling pathway that couples glucose metabolism to insulin secretion (Ashcroft et al., 1994).

## Material and Methods

### Cells

Unless stated otherwise, cells of the mouse pancreatic  $\beta$ -cell line MIN6 were employed (Miyazaki et al 1990). The MIN6 cell line is a well-established, time honored, model for the study of pancreatic  $\beta$ -cell function (Miyazaki et al., 1990; Ishihara et al., 1993; Daunt et al.,

2006; Cataldo et al., 2015). The main advantage of a cell line for pancreatic  $\beta$ -cell research is that it large numbers of phenotypically homogenous cells are available which are devoid of paracrine and neuroendocrine effects that arise from interaction with the other endocrine and neuronal cell types that reside within the pancreatic islet (Ishihara et al., 1993). Although MIN6 have been reported to contain and secrete other pancreatic endocrine hormones, these cells still remain primarily  $\beta$ -cell in function (Nakashima et al., 2009). Cells were grown, and the chronic experiments performed, in Dulbecco's modified Eagle's medium (DMEM) which contained 25 mM glucose and was supplemented with: 2 mM L-glutamine, 10% fetal calf serum, 50  $\mu$ M 2-mercaptoethanol and 25 mM HEPES. In this study cells from passage numbers 35-42 were used. Some experiments were repeated with the human pancreatic beta-cell line, 1.1B4 (McCluskey et al., 2011). These cells were maintained and handled using the same protocols as for MIN6. For validation in native tissue we used  $\beta$ -cells both from and within mouse islets of Langerhans. Pancreatic islets were isolated from the pancreata of male 30-35g CD1 mice as previously described (Daunt et al., 2006). Animals were kept under conditions and methods used that complied with local University rules approved by the UK government home office.

**Chronic studies**

**Measurement of cell viability with MTT**

The MTT (3-(4,5-dimethylthiazol-2-yl)-2,5-diphenyl tetrazolium bromide) assay relies on cellular reduction of the MTT substrate to produce a blue formazan product. As such it is a facile indicator of cell viability that results from the product of cell number and redox status (Elmorsy et al., 2014). The MTT assay was employed in accord with the manufacturer's protocol (CellTiter 96 Non-Radioactive Cell Proliferation Assay; Promega, UK). Cells were incubated for 4, 24, 48 or 72 hours in the presence of ADs or vehicle. In one set of experiments, this assay was repeated in the presence of 10 mM reduced glutathione (GSH) with a concentration of AD that inhibited MTT reduction by ~ 50% after 24 hours incubation (Elmorsy et al., 2014).

To account for inter-experimental variation between well cell densities, MTT absorbance values are expressed as a percent of that measured for its respective vehicle control (defined as 100%). For all chronic assays, each experiment was performed in triplicate (technical repeat) with the average value considered as a single biological repeat.

### **Intracellular ATP content**

As a direct measure of bioenergetic potential, intracellular ATP was measured as previously described (Elmorsy and Smith, 2015). Data was corrected for background luminescence by subtraction of the values measured in media alone. ATP levels are represented as a percentage measured in their respective vehicle control.

### **Insulin secretion**

For this and all subsequent chronic AD incubation assays, cells at confluence were washed twice with PBS and incubated for 24 hrs in DMEM with ADs or vehicle. To maximize effect detection, concentrations of ADs were chosen that inhibited MTT reduction/ATP production by ~ 50% after 24 hours incubation.

To measure insulin secretion, the media was removed and the cells washed with PBS. Cells were then incubated for 15 minutes in serum free DMEM (25 mM glucose) absent of AD. This was removed for insulin assay and the cells measured for total insulin content. Insulin was measured by ELISA (Crystal Chem, Downers Grove, IL, USA) with secretion normalized to total insulin content.

### **Lactate production**

To measure lactate in the chronic experiments the supernatant was collected and assayed by kit in accord with the manufacturer's instructions (Biovision, Mountain View, CA). Lactate production was normalized to cell number, estimated with a hemacytometer, and expressed as a percentage of lactate produced with the vehicle control.

### **Mitochondrial complex activity**

The effect of ADs on MIN6 cells mitochondrial complexes I and III were assessed as previously described (Elmorsy and Smith, 2015). To maximize event detection, concentrations of ADs were chosen that inhibited MTT reduction/ATP production by ~ 50% after 24 hours incubation.

### **Oxidative stress**

The 3,7-dichlorodihydrofluorescein diacetate (DCFDA) assay was used to detect reactive oxygen species (ROS) and was performed following the protocol of Elmorsy et al (2014). For a positive

control 1  $\mu$ M Antimycin A was added for 30 minutes, this blocks Complex III and generates of ROS. Non-stained cells were used for the blank and were subtracted from the data to correct for background luminescence.

**Caspase activity**

To determine if the ADs, may induce apoptosis we evaluated the activities of caspases 3, 8 and 9 after treatment with the ADs for 24 hrs. These were determined using a BD ApoAlert caspase fluorescent assay kits (Clontech Laboratories, Palo Alto, CA).

**Acute studies**

Unless stated otherwise, acute experiments were performed in a HEPES-buffered Hanks solution which contained (in mM): 138 NaCl, 4.2 NaHCO<sub>3</sub>, 1.2 NaH<sub>2</sub>PO<sub>4</sub>, 5.6 KCl, 1.2 MgCl<sub>2</sub>, 2.6 CaCl<sub>2</sub>, 10 HEPES (pH 7.4 with NaOH) and 0.01 % fatty acid free BSA.

**Mitochondrial respiratory rate: O<sub>2</sub> consumption**

The rate of O<sub>2</sub> consumption (OCR) of MIN6 and 1.1B4 cell suspensions were measured polarographically with a redox over potential of -0.625 V using Clark Oxygen Electrodes (Rank Brothers, Bottisham, UK) as described previously (Daunt et al., 2006). The background O<sub>2</sub> consumption by the electrode was corrected for by subtraction of the OCR measured after the addition of 6 mM Na azide which blocks Complex IV and mitochondrial respiration. Results obtained with the N,N,N',N'-tetramethyl-p-phenylenediamine (TMPD) and ascorbate electron shuttle system (ASB; Duchen et al., 1993; Daunt et al., 2006) were corrected for autoxidation of ascorbate via subtraction of the OCR obtained with ascorbate in the absence of cells: (0.3 nmol min<sup>-1</sup> in 1 ml chamber volume). To improve the statistical power for the substrate experiments, data was pooled from both control, and AD experiments, which resulted in different n numbers as indicated.

**Real time lactate production**

The rate of lactate production of MIN6 and 1.1B4 cell suspensions was measured simultaneously in conjunction with OCR. The appearance of lactate in the media was measured



polarographically with Sarissa Lactate enzyme Electrodes according to the manufacturer's protocol (Sarissa Biomedical Ltd Coventry, UK). The potential of the lactate electrode was set at +500 mV relative to a Ag/AgCl reference electrode (DriRef, WPI). At this potential the electrode oxidises  $\text{H}_2\text{O}_2$ , the product of lactate oxidation by lactate oxidase immobilised on the surface of a carbon fibre electrode; the resultant electrical current is a stoichiometric measure of lactate concentration. Electrode calibration was performed with known concentrations of lactate and was linear up to  $\sim 800 \mu\text{M}$  (Sarissa Biomedical Ltd). The lactate output of the cells was calculated after subtraction of the linear background leak current of the electrode measured in the absence of the acid ( $-1.38 \text{ nmol min}^{-1}$  in 4 ml chamber volume). Compounds were confirmed as not to interfere with the electrode by protocol repetition in the absence of cells.

### **Mitochondrial membrane potential**

The mitochondrial membrane potential,  $\Delta\Psi_{\text{mit}}$ , was monitored with Rhodamine-123 (Rh-123) similar to that described previously (Daunt et al., 2006). Only cells that responded to glucose with a decrease in fluorescence and an increase to the protonophore FCCP (carbonyl cyanide-4-(trifluoromethoxy)phenylhydrazone) were chosen for quantitative analysis. Regions of interest (ROI) were drawn around cells, corrected for background fluorescence by subtraction, and the average ROI fluorescence intensity calculated. ROIs were recorded for both single cells and cell clusters within each visual field. Only cells that responded to glucose (hyperpolarization of  $\Delta\Psi_{\text{mit}}$ ) were used for analysis. Image analysis was performed with custom scripts written in Labtalk (ORIGIN Ver, 6.0, OriginLab Corporation, MA USA).

### **Patch-clamp studies of $\text{K}_{\text{ATP}}$ channel activity**

As an indicator of sub-membrane ATP concentrations  $\text{K}_{\text{ATP}}$  channel activity was measured the with cell-attached patch-clamp technique as previously described (Ashcroft et al. 1988; Smith et al., 2001). Cells were bathed in a high potassium solution, nominally  $\text{Ca}^{2+}$  free, to electrochemically clamp the cell membrane potential ( $V_m$ ) to 0 mV. The pipette potential,  $V_p$ , was held at + 70 mV to clamp the trans-patch membrane potential to -70 mV:

$(V_m - V_p)$ . The pipette solution contained (in mM): 140 KCl,  $\text{CaCl}_2$  2.6,  $\text{MgCl}_2$  1.2, and HEPES 10 (pH 7.4 with NaOH). 100  $\mu\text{M}$  tetraethyl ammonium was added to block voltage-gated  $\text{K}^+$  channels. Patch pipettes, resistances between 2-4  $\text{M}\Omega$ , were drawn from GC150TF

capillary glass (Harvard Instruments), coated with dental wax (Kerr) and fire polished before use. Currents were measured using an Axopatch 1D patch clamp amplifier (Molecular Devices). The zero-current potential of the pipette was adjusted with the pipette in the bath just before seal establishment. No corrections have been made for liquid junction potentials (<4 mV). Currents were low pass filtered at 2 kHz (–3db, 8 pole Bessel) and digitized at 10 kHz using PClamp 9.3 (Axon Instruments, Foster City, USA). Single-channel data were analyzed with half-amplitude threshold techniques as implemented in Clampfit Ver. 10.6 (Axon Instruments, Foster City, USA). Channel activity, NPo, was recorded for 3 minute periods. These experiments were performed at 21-23 °C a temperature at which glucose metabolism (Dawson et al., 1986) and its ability to block KATP channels activity (Ashcroft et al., 1988; Smith et al; 2001) in beta-cells is maintained, albeit slower than at 37 °C.

**Mitochondrial superoxide**

To measure mitochondrial ROS and oxidative stress after acute AD incubation the fluorescent dye MitoSOX™ was employed in accord with the manufacturer’s instructions (ThermoFisher Scientific, Waltham MA USA). Cells cultured in 6-well plates to confluence were incubated in the dark with 5 μM MitoSOX reagent for 10 min at 37°C. Cells were then washed three times with PBS and incubated in Hanks solution with drugs for 120 min at 37°C. DMSO was used as the vehicle control, 1 μM antimycin A as the positive control and unstained cells for blank. Cells were then washed again with PBS and the dye excited at 510 nm. The emission at 580 nm was captured by fluorescence microscopy. After subtraction of the blank, the mean value of five random images from each well was taken as single sample. Velocity software (Ver. 6.3.1.0, Perkin Elmer Inc.) was used to analyze the fluorescent intensity of individual cells and clusters.

**Statistical analysis**

Statistical analysis and curve fitting was performed using Graphpad PRISM version 7.01 (San Diego, California USA). Data distributions were tested for normality with the D'Agostino & Pearson omnibus normality test and the appropriate statistical test used as given in the text. Inter-experimental variation within the assay are either indicated by plots of raw values or the coefficient of variation, CV.

The concentration-response relationships for the actions of ADs were quantified by fitting the assay data with equation 1:  $Y = (100 - pedestal) / (1 + ([AD] / IC_{50})^h)$

Where Y is the % of control (taken as 100%), pedestal is the minimum value for Y, h is the slope index, [AD] is the concentration of antidepressant and  $IC_{50}$  the concentration of drug that produces half-maximal inhibition. All the data generated was confirmed to best fit with a single rather than a two site binding model by the comparison method of Akaike's Information Criteria (Graphpad PRISM).

The relationship between incubation time and  $IC_{50}$  was quantified by fitting the data with the empirical equation 2:  $IC_{50, t} = (IC_{50, t=0} - \text{plateau}) \times \exp(-K \times t) + \text{plateau}$

Where  $IC_{50, t}$  is  $IC_{50}$  at time t in hours,  $IC_{50, t=0}$  is the  $IC_{50}$  at time 0, plateau is the asymptotic value of  $IC_{50}$  and K is the rate constant ( $\text{hours}^{-1}$ ). For the majority of the acute fluoxetine studies its  $IC_{50, t=0}$  value was used: 30  $\mu\text{M}$ .

Data are given in text as the mean  $\pm$  SEM or median with 5 to 95% confidence intervals (C.I.), with n the number of individual determinations as appropriate. Statistical significance is defined as  $P < 0.05$ . In graphics,  $P < 0.05$  is flagged as \*,  $P < 0.01$  as \*\*,  $P < 0.001$  as \*\*\* and  $P < 0.0001$  as \*\*\*\*. Statistical tests are stated in the text and figure legends where appropriate.

## Results

### Chronic studies

The ability of MIN6 to reduce MTT was maintained up to 72 hours, the longest period used (Fig. 1A); in control cells there was no change in MTT reduction with time (Pearson  $r = 0.79$ ,  $-0.71$ -1 95% C.I;  $p=0.21$ ), indicative of little cell replication over this time frame. Inter-experimental variation was small and ranged between 2.2 to 4.7 % ( $n = 9$ ). Figs. 1B-D illustrates that paroxetine, fluoxetine and clomipramine inhibited the ability of MIN6 to reduce MTT in a time and concentration manner. Equation 1 was best fit to the data with  $IC_{50}$  and pedestal values given in Figs. 1E and F ( $h \sim 0.5$ ). The maximum amount of block, as indicated by the decrease in pedestal, significantly increased with incubation time for both paroxetine (F test,  $p < 0.005$ ) and clomipramine (F test,  $p < 0.0001$ ) but not fluoxetine (Fig. 1F). Only the  $IC_{50}$  value for fluoxetine showed a significant change in magnitude with time of incubation (F test,  $p < 0.0001$ ; Figs. 1E) and was described by equation 2 with an  $IC_{50, t=0}$  of 33  $\mu\text{M}$  (12 to 53, 95% C.I.), a plateau of 4.7  $\mu\text{M}$  (0 to 9.5, 95% C.I.) and a K of 0.1  $\text{hours}^{-1}$  (0 to 2.8, 95% C.I.). Fig. 1G demonstrates that a significant block of MTT reduction occurred with all three ADs at 100 nM, the lowest concentration used (One sample t test relative to vehicle control) at all incubation times. Fig. 1H

illustrates that co-incubation with 10 mM GSH partially reversed the inhibition of MTT reduction produced by the ADs.

Fig. 2 shows that intracellular ATP production, like MTT reduction, was inhibited in a concentration-dependent manner after 24 hour exposure to AD. Inter-experimental variation ranged from 1.7% CV for control up to 1.8 % CV in the presence of fluoxetine (n = 9). Equation 1 was readily fit to the data with the same  $IC_{50}$ 's given in Fig. 2D. For each AD tested no significant difference (ANOVA) was found between the  $IC_{50}$  for MTT and ATP; data when combined with the fact that cell density (Fig 3F) did not change suggests that MTT is measuring redox status and not viability. All three ADs decreased the activity of both complex I and III (Fig. 2E and D; One sample t test relative to control). Inter-experimental variation as indicated by the CV ranged from 5% for control up to 18 % for Complex III in the presence of clomipramine (n = 3).

Since these ADs decreased the activities of Complexes I and III, and also impaired the ability of MIN6 cells to reduce MTT and produce ATP, we investigated whether the drugs could affect glycolysis via measurement of their lactate output as well as generate ROS. Figs. 3A and B illustrate that paroxetine, fluoxetine and clomipramine all significantly increased lactate output and ROS when normalized to their respective controls (One sample t-test relative to 100%). However, a slightly different picture was observed when inter-plate variability was not controlled for and raw data was used instead (Figs. 3C &D), with significant effects only observed for fluoxetine when compared to its respective control (ANOVA with Dunnett's).

A prior 24 hour incubation in paroxetine and fluoxetine, at concentrations estimated to produce ~ 50% inhibition of MTT reduction/ATP production, significantly decreased the ability of the MIN6 cells to secrete insulin (Fig. 3D, One sample t-test relative to control: 100%), however this treatment did not affect cell density (Fig. 3F). Similar conditions significantly increased the activity of caspases 3, 8 and 9 (Fig.3G)

### Acute studies

As it is not readily possible to measure cellular redox potential via MTT reduction or cellular bioenergetics via ATP production over incubation times of minutes, these parameters were monitored instead by the rate of respiration (OCR) and mitochondrial membrane potential,  $\Delta\psi_{mit}$ , respectively (Duchen et al., 1993). Acute actions of these drugs are in keeping with accidental drug overdose, loading dosage or short term drug-drug interactions.

MIN6 suspensions consumed  $O_2$  (OCR) at a rate commensurate with cell density at  $1.3 \pm 0.7$  nmoles  $10^6$  cells $^{-1}$  min $^{-1}$  ( $n = 112$ ). Addition of 10 mM glucose produced a  $\sim 1.4$  fold increase in OCR to  $1.7 \pm 0.8$  nmoles  $10^6$  cells $^{-1}$  min $^{-1}$  ( $n = 112$ ), subsequent addition of fluoxetine significantly decreased OCR (Figs. 4A, 4C). This effect was concentration-dependent with an  $IC_{50}$  of 230  $\mu M$  (139 to 397, 95% C.I.) and  $h$  of 1.1 (0.6 to 1.6, 95% C.I.; Fig. 4D solid line). After only 10 minutes incubation, 3  $\mu M$  was the lowest concentration of fluoxetine to have a significant effect on OCR (Kruskal-Wallis, Dunn's multiple comparison test). Similar observations were made in the human beta-cell line 1.1B4 with an  $IC_{50}$  for fluoxetine of 232  $\mu M$  (53 to 102, 95% C.I.) and  $h$  of 0.8 (0.4 to 1.2, 95% C.I.; Fig. 4D solid line). The apparent potency of the SSRI to inhibit OCR in MIN6 was increased in 100 nM FCCP (F-test,  $P < 0.04$ ; Fig. 4C), with an  $IC_{50}$  of 97  $\mu M$  (81-117, 95% C.I.) and  $h$  of 1.9 (0.9-2.8, 95% C.I.; data not shown). Acutely applied paroxetine failed to affect OCR even up to 100  $\mu M$ , the highest concentration tested (data not shown) whereas clomipramine inhibited OCR with an  $IC_{50}$  of 284  $\mu M$  (319-372, 95% C.I.) and  $h$  of 1.5 (0.87-2, 95% C.I.) with 30  $\mu M$  the lowest concentration that had a significant effect after 10 minute incubation (Kruskal-Wallis, Dunn's multiple comparison test; data not shown).

To confirm that the acute effect of fluoxetine on  $O_2$  consumption was not unique to cell lines, its effect on mouse pancreatic islets was tested. In the absence of exogenous substrate, pancreatic islets consumed  $O_2$  at  $1.9 \pm 0.5$  pmol  $O_2$  islet $^{-1}$  min $^{-1}$  ( $n = 6$ ). The addition of 20 mM glucose significantly increased OCR  $\sim 1.6$  fold to  $3.0 \pm 0.4$  pmol  $O_2$  islet $^{-1}$  min $^{-1}$  ( $p < 0.05$ ; ANOVA, Sidaks's multiple comparison test; Fig. 4D); values akin to those previously reported (Daunt et al., 2006). Incubation in 100  $\mu M$  fluoxetine for 10 minutes significantly inhibited OCR by 54 % to  $1.6 \pm 0.3$  pmol  $O_2$  islet $^{-1}$  min $^{-1}$  ( $p < 0.01$ ; ANOVA, Sidaks's multiple comparison test); a magnitude of block larger than that observed for MIN6 cells at the same drug concentration (33%; Unpaired t test with Welch's correction) and suggests an  $IC_{50}$  of  $\sim 100$   $\mu M$  for fluoxetine in the intact islet..

To explore candidate target sites for the acute effect of fluoxetine on beta-cell metabolism, a range of substrates which feed in at different entry points of the catabolic pathway for glucose, stimulate OCR and elicit insulin secretion (Daunt et al., 2006) were tested for their susceptibility to inhibition by this SSRI. These were D-glyceraldehyde, methylpyruvate and  $\alpha$ -ketoisocaproate (all at 10 mM), and the electron shuttle TMPD/ascorbate (ASB) (Duchen et al., 2003). Of these, only glyceraldehyde did not stimulate OCR relative to the osmotic control, 10 mM 3-O-methyl glucose, (MOG; Fig. 5A; Kruskal-Wallis, Dunn's multiple comparison test). Within 10 minutes of incubation, 30  $\mu$ M fluoxetine inhibited respiration in the presence of all these substrates, except MOG where the block failed to reach significance, an effect regardless of the substrates' ability to stimulate OCR (Fig. 5B; Mann Whitney test relative to respective vehicle control in each substrate).

Although the magnitude of block produced by fluoxetine was unrelated to the change in OCR produced by substrate, it was positively correlated with the magnitude of basal OCR (Spearman  $r$ , Fig. 5C). This is exemplified in Fig. 5D, with the greatest inhibition produced by 30  $\mu$ M fluoxetine was in cell suspensions with the largest basal OCR (Spearman  $r = 0.64$ ,  $p < 0.0001$ ). This phenomenon was further explored with different glucose concentrations (Fig. 5E and F). Fig. 5E illustrates that a significant decrease in OCR occurred with fluoxetine ( $76\% \pm 2.6\%$ ;  $p < 0.001$  for all cases, paired Student's  $t$ -test); an effect independent of glucose concentration and the OCR stimulated by the sugar (Spearman  $r = 0.04$ ,  $p \sim 0.5$ ). Because the magnitude of the SSRI effect is independent of glucose concentration, when the effect of the drug is plotted as a % of the OCR measured in glucose, the inhibitory effect of the AD appears to be negatively correlated with the concentration of sugar (Fig. 5F; Spearman  $r = -0.96$ ,  $p < 0.01$ ); with the SSRI appearing apparently less efficacious at the larger rates of respiration associated with higher glucose concentrations.

Fig. 6 demonstrates that 10 mM glucose increased lactate production commensurate with an increase in OCR. Subsequent inhibition of OCR with 30  $\mu$ M fluoxetine was associated with an increment in lactate output (Fig. 6A, B). The ability of fluoxetine to block OCR and stimulate lactate output was mimicked by 1  $\mu$ M rotenone (Fig. 6C, D), with OCR blocked beyond basal in some cases. Fluoxetine at 30  $\mu$ M also inhibited OCR and simulated lactate output in the human

beta-cell line, 1.1B4 (Fig. 6E, F). These effects were significantly larger than those seen in MIN6 cells, a fact due to the greater rate of glucose utilization by 1.1B4.

Fig. 7A shows that in the absence of exogenous substrate the mitochondrial membrane potential,  $\Delta\Psi_{mit}$ , as indicated by Rh123 fluorescence, was stable. Within one minute of 10 mM glucose addition, a sustained decrease in fluorescence occurred; an effect consistent with energization of the mitochondria and polarization of  $\Delta\Psi_{mit}$  associated with enhanced mitochondrial electron transport due to glucose metabolism (Duchen et al., 1993). Application of 2.5  $\mu\text{g ml}^{-1}$  oligomycin decreased fluorescence consistent with an increase in  $\Delta\Psi_{mit}$  due to the block of  $\text{H}^+$  leakage through the  $\text{F}_0\text{-F}_1\text{-ATPase}$  (Duchen et al., 1993). Subsequent addition of 1  $\mu\text{M}$  antimycin increased Rh123 fluorescence; an observation consistent with the abolition of mitochondrial electron transport and collapse of  $\Delta\Psi_{mit}$  since subsequent addition of 1  $\mu\text{M}$  of the mitochondrial protonophore FCCP did not elicit a further increase in fluorescence (Fig. 7A). Fig. 7B shows that after energization of  $\Delta\Psi_{mit}$  with glucose, 30  $\mu\text{M}$  fluoxetine increased Rh123 fluorescence; however, the depolarization of  $\Delta\Psi_{mit}$  produced by fluoxetine was incomplete as demonstrated by the collapse of  $\Delta\Psi_{mit}$  that occurred on the addition of 1  $\mu\text{M}$  FCCP. Addition of 1  $\mu\text{M}$  rotenone, like antimycin A, depolarized  $\Delta\Psi_{mit}$ , and prevented further dissipation of  $\Delta\Psi_{mit}$  by 30  $\mu\text{M}$  fluoxetine and 1  $\mu\text{M}$  FCCP (Fig. 7C).  $\text{H}_2\text{O}$ , the vehicle for fluoxetine, did not affect Rh123 fluorescence, whereas 1  $\mu\text{M}$  FCCP could still collapse  $\Delta\Psi_{mit}$  (Fig. 7D). Since the absolute value of  $\Delta\Psi_{mit}$  reflects a balance between its generation by electron transport and its dissipation, predominantly via  $\text{F}_0\text{-F}_1\text{-ATPase}$  activity (Duchen et al., 2003), the ability of an agent to depolarize  $\Delta\Psi_{mit}$  can be due to either inhibition of its generation or/and potentiation of its dissipation. On the basis of the retained ability of fluoxetine to inhibit OCR in the presence of FCCP, we assumed the former and quantified the action of fluoxetine on  $\Delta\Psi_{mit}$  by its initial rate of effect ( $\Delta\text{Rh123}$ ; Fig. 7E).  $\Delta\text{Rh123}$  was positively associated with drug concentration (Pearson  $r = 0.972$ ,  $p < 0.01$ ), with 10  $\mu\text{M}$  the lowest fluoxetine concentration deemed to have a significant effect (ANOVA, Dunnett's post comparison test). Although 30  $\mu\text{M}$  fluoxetine depolarized  $\Delta\Psi_{mit}$  relative to  $\text{H}_2\text{O}$ , the vehicle control ( $p < 0.01$ , Kruskal-Wallis Dunn's multiple comparison test), the magnitude of this effect was unrelated to the extent by which glucose energized  $\Delta\Psi_{mit}$  (Pearson  $p > 0.3$ ), nor did it reverse the effect of glucose on  $\Delta\Psi_{mit}$  (Fig. 7F).

Fig. 8 shows that 1  $\mu$ M Antimycin A after 30 minutes, but not 30  $\mu$ M fluoxetine after 120 minutes, significantly increased ROS in MIN6 cells relative to vehicle control (DMSO;  $p < 0.001$ , ANOVA Holm-Sidak).

**FCCP, but not fluoxetine reactivates  $K_{ATP}$  channel activity**

Fig. 9A show that in the absence of glucose, cell-attached patches displayed single-channel currents with biophysical metrics characteristic for  $K_{ATP}$ -channels: a single channel current amplitude ( $i$ ) of  $4.8 \pm 0.1$  pA, burst kinetics and a mean open-channel dwell time of  $2.2 \pm 0.1$  ms ( $n = 27-37$ ; Ashcroft et al. 1988; Smith et al., 2001). Fig. 9A and 9B shows that addition of 10 mM glucose significantly reduced NPo by 99% (42 to 0%, 95% C.I;  $p < 0.0001$  Wilcoxon Signed rank test,  $n = 46$ ) relative to the perfusion control that was without effect (Wilcoxon Signed rank test,  $n = 10$ ). Fluoxetine (1-100  $\mu$ M) failed to reactivate  $K_{ATP}$  channel activity blocked by glucose, even after 10 minutes the longest period tested (Figs. 9A, 9C). Although 1  $\mu$ M rotenone, a mitochondrial toxin which mimics the metabolic effects of fluoxetine, nor 1  $\mu$ M antimycin failed to reactivate the channel, 100 nM FCCP did (Kruskal-Wallis; Fig 9A and 9C) confirmed by the subsequent abolition of activity with 20  $\mu$ M tolbutamide, a potent selective inhibitor of this channel type (Smith et al., 2001).

**Discussion**

*Antidepressants are cytotoxic to MIN6*

Since all three ADs decreased MTT reduction and ATP levels, effects with similar  $IC_{50}$ s without affecting cell density which suggest ADs act to impair redox status. Previous studies have demonstrated that fluoxetine (Caminada et al., 2006; Levkovitz et al., 2005; Krishnan et al., 2008), clomipramine (Levkovitz et al., 2005; Abdel-Razaq et al., 2011) and paroxetine (Amit et al. 2009) inhibit cell metabolism with  $IC_{50}$  values similar to those we report. Although these  $IC_{50}$ 's exceed therapeutic concentrations, all three drugs produced cytotoxic effects at the therapeutically relevant concentration of 100 nM. Despite intra-islet concentrations for these drugs being unavailable, magnetic resonance spectroscopy of  $^{19}F$  fluoxetine in the human brain has revealed a 10-20 fold accumulation of fluoxetine ( $\sim 13 \mu$ M) relative to plasma after 6-12 months treatment (Karson et al 1993; Bolo 2000), Together, these findings help explain the



diabetogenic risk associated with prolonged AD usage and exposure (Lustman et al., 1997; Rubin et al., 2008; Brown et al., 2008; Derijks et al., 2008; Andersohn et al., 2009; Kivimäki et al., 2010; Khoza et al., 2011).

#### *AD effects are not mediated by blockade of serotonin transport*

Fluoxetine and paroxetine are SSRIs, whereas clomipramine acts as an SSRI and a noradrenaline re-uptake inhibitor. These drugs are thought to achieve their antidepressant therapeutic activity, in part, through blockade of the serotonin transporter (SERT) which enhances serotonin (5-HT) concentrations in the brain to alleviate the symptoms of depression (Blier & El Mansari, 2013). Pancreatic  $\beta$ -cells secrete 5-HT which may exert autocrine effects (Bennet et al., 2015). However, an involvement of SERT for the cytotoxic effects of these ADs can be dismissed, since  $\beta$ -cells do not express the Slc64a gene that encodes for SERT nor do ADs affect the release of 5-HT from them (Cataldo et al., 2015).

#### *Antidepressants impair $\beta$ -cell mitochondrial function*

The  $IC_{50}$  for the inhibition of oxidative respiration by acute application of fluoxetine on intact  $\beta$ -cells is comparable to that seen in isolated mitochondria from liver ( $\sim 300 \mu M$ ; Souza et al., 1994) and brain ( $\sim 150 \mu M$ ; Curti et al., 1999) both for this drug and its metabolite norfluoxetine. Furthermore, Hroudová et al (2012) reports that fluoxetine inhibits Complex 1 and II with  $IC_{50}$ 's of 86 and 266  $\mu M$  respectively. Other mitochondrial targets for fluoxetine are the  $F_0F_1$ -ATPase (Souza et al., 1994; Curti et al., 1999) and the voltage-dependent anion channel, VDAC (Nahon et al., 2005). However, neither of these proteins are likely targets here since when the activity of  $F_0F_1$ -ATPase was uncoupled from mitochondrial electron transport by FCCP, the  $IC_{50}$  for fluoxetine was not increased; whereas blockade of VDAC by fluoxetine is associated with an enhanced, not impaired, mitochondrial function (Nahon et al., 2005).

The fact that the acute  $IC_{50}$  values exceeded the chronic values ones probably reflect a failure of the ADs to reach equilibrium over the short time periods employed. This is exemplified by fluoxetine whose affinity increased with incubation time with a half-life of 6.9 hrs.

The observations that the chronic AD bioenergetic effects were not associated with changes in cell density is consistent with a decrease in cell oxidative respiration capacity; an idea supported

by the loss of mitochondrial Complexes seen in other systems: 30% decrease in Complex IV in the  $\beta$ -cell line INS1E with 48 hour exposure to 1  $\mu$ M fluoxetine (De Long et al., 2014); >20% decrease for all four Complexes in CHO cells after 18 hour incubation with >10  $\mu$ M clomipramine (Abdel-Razaq et al., 2011). Moreover, at 1  $\mu$ M, the atypical AD bupropion, an AD associated with an increased risk of diabetes (Andersohn et al., 2009), impairs mitochondrial Complex IV function and insulin secretion in INS1E cells after 48 hour exposure (Woynilowicz et al., 2012). Complex I and complex III inhibition is considered the main source of ROS in cells (Ježek et al., 2005; Chen et al., 2003). Such a process was demonstrated in our chronic but not acute studies, an effect previously observed in INS1E cells when incubated with fluoxetine (De Long et al., 2014). These data suggest that maintained loss of mitochondrial Complex activity and ROS production only occurs with prolonged AD exposure; effects similar to those observed in  $\beta$ -cells with exogenous  $H_2O_2$  (Li et al., 2009).

*Fluoxetine blocks  $\beta$ -cell lipid metabolism*

In the absence of exogenous substrate pancreatic  $\beta$ -cells respire primarily via beta-oxidation of endogenous lipids (Corkey et al., 1989) which involves FADH and Complex II/III. The observation that acute fluoxetine had an effect size correlated with basal, rather than stimulated, respiration lends support to Complex II/III as an acute target for this AD; since inhibition of Complex II/III will prevent beta-oxidation of endogenous lipids and OCR. Indeed, fluoxetine mimics the antimycin inhibition of Complex II/III on  $\Delta\Psi_{mit}$ . A mitochondrial target for fluoxetine is supported by the increase in lactate production that occurs with this SSRI, a phenomenon, like that produced by rotenone, explained by a failure of the beta-cell to oxidize NADH via Complex I which necessitates NADH recycling via increased lactate generation from pyruvate. An event that help maintains cytosolic ATP and  $K_{ATP}$  channel block.

*Antidepressants decrease insulin secretion by MIN6*

The decrease in glucose-stimulated insulin secretion may be due to a combination of both oxidative stress and decreased ATP production. Pancreatic  $\beta$ -cells are characterized by a relatively weak expression of superoxide dismutase, catalase and glutathione peroxidase (Grankvist et al., 1996; Lenzen et al., 1996); enzymes that metabolize and neutralize ROS. Consequently, exposure to oxidative stress as is the case here, may be sufficient to impair

glucose-stimulated insulin secretion (Maechler et al., 1999; Sakai et al., 2003; Li et al., 2009). The finding that co-incubation with GSH partially reversed the ability of AD to inhibit MTT reduction is consistent with this notion. The associated suppression of intracellular ATP due to bioenergetic disruption will also act to decrease insulin secretion as it is the major coupling factor for glucose-induced insulin secretion (Smith et al., 1989; Eliasson et al., 1997) and help explains their ability to induce hyperglycaemia without hyperinsulinaemia in vivo (Yamada et al., 1999; Gomez et al., 2001).

#### *Fluoxetine fails to activate $K_{ATP}$ channels in MIN6*

Plasma-membrane  $K_{ATP}$  channel activity was blocked by glucose and solely reactivated by FCCP; however, they were not reactivated by fluoxetine, rotenone or antimycin. This is because these compounds failed to impair mitochondrial ATP production sufficiently to reactivate  $K_{ATP}$ ; unlike FCCP which uncouples respiration and leads to cellular consumption of ATP via reverse mode  $F_0F_1$ -ATPase activity (Rustenbeck et al., 1997). Rotenone and antimycin are well-known to inhibit insulin secretion independently of  $K_{ATP}$  channels due to the intimate relationship between mitochondrial metabolism and secretory steps distal to membrane ionic events (MacDonald & Fahien, 1990; Ortsäter et al., 2002), and as we show here fluoxetine, too can also impair mitochondrial respiration acutely which explains its acute hyperglycemic affects in-vitro (Antoine et al., 2004; Cataldo et al., 2015) and in-vivo (Yamada et al., 1999; Gomez et al., 2001); effects mediated by the energetic requirements of distal events in secretion such as  $Ca^{2+}$  entry (Smith et al., 1989) and exocytosis (Eliason et al., 1997).

#### *Suitability of MIN6 as a metabolic model of native pancreatic beta-cells*

We found that glucose stimulated MIN6 OCR 1.4 fold that of basal, close to that of 1.6 observed for mouse islets. Furthermore, the MIN6 cell OCR of  $1.7 \text{ nmol } 10^6 \text{ cells}^{-1} \text{ min}^{-1}$  in glucose is similar to that of  $3 \text{ nmol } O_2 \text{ } 10^6 \text{ cells}^{-1} \text{ min}^{-1}$  in mouse islets (Daunt et al., 2006). Moreover, the  $2.6 \text{ nmol min}^{-1} 10^6 \text{ cell}$  lactate from MIN6 in 10 mM glucose is similar to that for rat islets:  $2.0 \text{ nmol min}^{-1} 10^6 \text{ cell}$  (Sener et al., 1976). Furthermore, we estimate a lactate to OCR ratio of  $3.6 \pm 1$  ( $n = 8$ ) in MIN6, similar to that reported for rat  $\beta$ -cells (2.4; Sener et al., 1976). Together, these data support MIN6 cells as a suitable metabolic model of native  $\beta$ -cells in which to study mitochondrial function.

*Conclusion and clinical implications*

We found that paroxetine, clomipramine and fluoxetine were cytotoxic to mouse pancreatic  $\beta$ -cells, an effect dependent on concentration and exposure duration. Two effects were determined: an immediate direct block of mitochondrial Complex activity followed by a longer term loss of Complex activity associated with increased ROS. Importantly, adverse metabolic effects were seen at chronic AD concentrations of 100 nM; a value less than the median therapeutic concentration for most dosage regimens (Reis et al., 2009). Moreover, as the plasma concentration for these ADs are well established to be related to dose (Reis et al., 2009), a daily fluoxetine dose of 80 mg can yield steady state plasma concentrations  $>2 \mu\text{M}$  (Lundmark et al., 2001); a concentration sufficient to disrupt beta-cell mitochondrial bioenergetics. Indeed, plasma concentrations during loading and drug-drug interactions concentrations may surpass  $2 \mu\text{M}$ . Why these ADs seem to have adverse clinical affects manifested predominantly by pancreatic  $\beta$ -cell dysfunction probably relates to the poor antioxidant abilities of this cell type, since they were mitigated in part by GSH. Overall, our data suggests that a direct cytotoxic effect of these ADs on pancreatic  $\beta$ -cells may contribute to the diabetogenic potential of antidepressants.

*Conflict of interest*

The authors declare that they have no conflict of interest

**References:**

Abdel-Razaq, W., Kendall, D.A. and Bates, T.E. (2011) The effects of antidepressants on mitochondrial function in a model cell system and isolated mitochondria. *Neurochem Res.* 36, 327-338

Andersohn, F., Schade, R., Suissa, S. and Garbe, E. (2009) Long-Term Use of Antidepressants for Depressive Disorders and the Risk of Diabetes Mellitus *Am J Psychiat* 166, 591–598.

Antoine, M.H., Gall, D., Schiffmann, S.N. and Lebrun, P. (2004) Tricyclic antidepressant imipramine reduces the insulin secretory rate in islet cells of Wistar albino rats through a calcium antagonistic action. *Diabetologia* 47, 909-916

- Amit, B.H., Gil-Ad, I., Taler, M., Bar, M., Zolokov, A. and Weizman, A. (2009) Proapoptotic and chemosensitizing effects of selective serotonin reuptake inhibitors on T cell lymphoma/leukemia (Jurkat) in vitro. *Euro. Neuropsychopharm.* 19, 726-734
- Ashcroft, F.M., Ashcroft, S.J. and Harrison, D.E. (1988) Properties of single potassium channels modulated by glucose in rat pancreatic beta-cells. *J. Physiol.* 400, 501-527
- Ashcroft, F.M., Proks, P., Smith, P.A., Ammala, C., Bokvist, K. and Rorsman, P. (1994) Stimulus-secretion coupling in pancreatic beta cells. *J. Cell. Biochem.* 55 Suppl, 54-65
- Bennet, H., Balhuizen, A., Medina, A., Nitert, M.D., Laakso, E.O., Essén, S., Spégel, P., Storm, P., Krus, U., Wierup, N. and Fex, M. (2015). Altered serotonin (5-HT) 1D and 2A receptor expression may contribute to defective insulin and glucagon secretion in human type 2 diabetes. *Peptides* 71, 113-120
- Blier, P., & El Mansari, M. (2013). Serotonin and beyond: therapeutics for major depression. *Phil. Trans. R. Soc. B*, 368(1615), 20120536.
- Bolo, N.R., Hodé, Y., Nédélec, J.F., Lainé, E., Wagner, G. and Macher, J.P. (2000) Brain pharmacokinetics and tissue distribution in vivo of fluvoxamine and fluoxetine by fluorine magnetic resonance spectroscopy. *Neuropsychopharm* 23, 428-438.
- Brown, L.C., Majumdar, S.R. and Johnson, J.A. (2008) Type of antidepressant therapy and risk of type 2 diabetes in people with depression. *Diabetes. Res. Clin. Pr.* 79, 61–67
- Caminada, D., Escher, C. and Fent, K. (2006) Cytotoxicity of pharmaceuticals found in aquatic systems: comparison of PLHC-1 and RTG-2 fish cell lines. *Aquat. Toxicol.* 79, 114-123.
- Cataldo, L.R., Cortés, V.A., Mizgier, M.L., Aranda, E., Mezzano, D., Olmos, P., Galgani, J.E., Suazo, J., and Santos, J.L. (2015) Fluoxetine impairs insulin secretion without modifying extracellular serotonin levels in MIN6  $\beta$ -cells. *Exp. Clin. Endocrinol.* 123, 473-478
- Chan, K., Truong, D., Shangari, N. and O'Brien, P.J. (2005) Drug induced mitochondrial toxicity. *Expert Opin. Drug Met.* 1, 655–669
- Chen, Q., Vazquez, E.J., Moghaddas, S., Hoppel, C.L. and Lesnefsky, E.J. (2003) Production of reactive oxygen species by mitochondria: central role of complex III. *J. Biol. Chem.* 278, 36027-36031
- Corkey, B.E., Glennon, M.C., Chen, K.S., Deeney, J.T., Matschinsky, F.M. and Prentki, M. (1989) A role for malonyl-CoA in glucose-stimulated insulin secretion from clonal pancreatic beta-cells. *J. Biol. Chem.* 264, 21608-21612

- Curti, C., Mingatto, F.E., Polizello, A.C., Galastri, L.O., Uyemura, S.A. and Santos, A.C. (1999) Fluoxetine interacts with the lipid bilayer of the inner membrane in isolated rat brain mitochondria, inhibiting electron transport and F1F0-ATPase activity. *Mol. Cell. Biochem.* 199, 103-109
- Daley, E., Wilkie, D., Loesch, A., Hargreaves, I.P., Kendall, D.A., Pilkington, G.J. and Bates, T.E. (2005) Chlorimipramine: a novel anticancer agent with a mitochondrial target. *Biochem. Bioph. Res. Co.* 328, 623-632
- Daunt, M., Dale, O. and Smith, P.A. (2006) Somatostatin inhibits oxidative respiration in pancreatic  $\beta$ -cells. *Endocrinology* 147, 1527-1535
- Dawson, C.M., Lebrun, P., Herchuelz, A., Malaisse, W.J., Gonçalves, A.A. and Atwater, I., (1986) Effect of temperature upon potassium-stimulated insulin release and calcium entry in mouse and rat islets. *Horm. Metabol. Res* 18, 221-224.
- Derijks, H.J., Heerdink, E.R., De Koning, F.H., Janknegt, R., Klungel, O.H. and Egberts, A.C. (2008) The association between antidepressant use and hypoglycaemia in diabetic patients: a nested case-control study. *Euro. J. Clin. Pharm.* 64, 531-538
- Duchen, M.R., Smith, P.A. and Ashcroft, F.M. (1993) Substrate-dependent changes in mitochondrial-function, intracellular free calcium-concentration and membrane channels in pancreatic beta-cells. *Biochem. J.* 294, 35-42
- Eliasson, L., Renström, E., Ding, W. G., Proks, P. and Rorsman, P. (1997). Rapid ATP-Dependent Priming of Secretory Granules Precedes  $\text{Ca}^{2+}$ -Induced Exocytosis in Mouse Pancreatic B-Cells. *J. Physiol* 503, 399-412.
- Elmorsy, E., Elzalabany, L.M., Elsheikha, H.M. and Smith, P.A. (2014) Adverse effects of antipsychotics on micro-vascular endothelial cells of the human blood–brain barrier. *Brain. Res.* 1583, 255-268
- Elmorsy, E. and Smith, P.A. (2015) Bioenergetic disruption of human micro-vascular endothelial cells by antipsychotics. *Biochem. Bioph. Res. Co.* 460, 857-862
- Eto, K., Fukuda, T., Araki, Y., Inoue, B. and Ogata, M. (1985) Effect of tricyclic drugs on mitochondrial membrane. *Acta. Med. Okayama.* 39, 289-295
- Gomez, R., Huber, J., Tombini, G. and Barros, H.M.T. (2001) Acute effect of different antidepressants on glycemia in diabetic and non-diabetic rats. *Braz. J. Med. Biol Res.* 34, 57-64

- Grankvist, K., Marklund, S.L. and Taljedal, I.B. (1981) CuZn-superoxide dismutase, Mn-superoxide dismutase, catalase and glutathione peroxidase in pancreatic islets and other tissues in the mouse. *Biochem. J.* 199, 393-398
- Hroudová, J. and Fišar, Z. (2012) In vitro inhibition of mitochondrial respiratory rate by antidepressants. *Toxicol. Lett.* 213, 345-352
- Ishihara, H., Asano, T., Tsukuda, K., Katagiri, H., Inukai, K., Anai, M., Kikuchi, M., Yazaki, Y., Miyazaki, J. and Oka, Y. (1993). Pancreatic  $\beta$ -cell line MIN6 exhibits characteristics of glucose metabolism and glucose-stimulated insulin secretion similar to those of normal islets. *Diabetologia* 36, 1139–1145
- Ježek, P. and Hlavatá, L. (2005) Mitochondria in homeostasis of reactive oxygen species in cell, tissues, and organism. *Int. J. Biochem. Cell.* 37, 2478-2503
- Joint Formulary Committee (2016) Fluoxetine In *British National Formulary*. 70. London: BMJ Group and Pharmaceutical Press
- Karson, C.N., Newton, J.E., Livingston, R., Jolly, J.B., Cooper, T.B., Sprigg, J. and Komoroski, R.A. (1993) Human brain fluoxetine concentrations. *J Neuropsychiatry Clin Neurosci* 5, 322-322.
- Kivimäki, M., Hamer, M., Batty, G.D., Geddes, J.R., Taba, A.G., Pentti, J., Virtanen, M. and Vahtera, J. (2010) Antidepressant Medication Use, Weight Gain, and Risk of Type 2 Diabetes. *Diabetes Care* 33, 2611–2616
- Khoza, S. and Barner, J.C. (2011). Glucose dysregulation associated with antidepressant agents: an analysis of 17 published case reports. *Int. J. Clin. Pharm.* 33, 484-492
- Krishnan, A., Hariharan, R., Nair, S.A. and Pillai, M.R. (2008). Fluoxetine mediates G0/G1 arrest by inducing functional inhibition of cyclin dependent kinase subunit (CKS)1. *Biochem. Pharmacol.* 75, 1924-1934
- Lenzen, S., Drinkgern, J. and Tiedge, M. (1996) Low antioxidant enzyme gene expression in pancreatic islets compared with various other mouse tissues. *Free. Radical. Bio. Med.* 20, 463-466
- Levkovitz, Y., Gil-Ad, I., Zeldich, E., Dayag, M. and Weizman, A. (2005) Differential induction of apoptosis by antidepressants in glioma and neuroblastoma cell lines: evidence for p-c-Jun, cytochrome c, and caspase-3 involvement. *J. Mol. Neurosci.* 27, 29-42

- Li, Y., Couch, L., Higuchi, M., Fang, J.L. and Guo, L. (2012) Mitochondrial dysfunction induced by sertraline, an antidepressant agent. *Toxicol. Sci.* 127, 582-591
- Li, N., Brun, T., Cnop, M., Cunha, D.A., Eizirik, D.L. and Maechler, P. (2009) Transient oxidative stress damages mitochondrial machinery inducing persistent beta-cell dysfunction. *J. Biol. Chem.* 284, 23602-23612
- De Long, N.E., Hyslop, J.R., Raha, S., Hardy, D.B. and Holloway, A.C. (2014) Fluoxetine-induced pancreatic beta cell dysfunction: New insight into the benefits of folic acid in the treatment of depression. *J. Affect. Disorders.* 166, 6-13
- Lundmark, J., Reis, M., & Bengtsson, F. (2001). Serum concentrations of fluoxetine in the clinical treatment setting. *Therapeutic drug monitoring*, 23(2), 139-147
- Lustman, A.J., Griffith, L.S., Clouse, R.E., Freedland, K.E., Eisen, S.A., Rubin, H., Carney, R.M. and McGill, J.B. (1997) Effects of Nortriptyline on Depression and Glycemic Control in Diabetes: Results of a Double-Blind, Placebo-Controlled Trial. *Psychosom. Med.* 59, 241-250
- MacDonald, M. J., & Fahien, L. A. (1990). Insulin release in pancreatic islets by a glycolytic and a Krebs cycle intermediate: contrasting patterns of glyceraldehyde phosphate and succinate. *Archives of Biochemistry and Biophysics*, 279(1), 104-108.
- Maechler, P. (2002) Mitochondria as the conductor of metabolic signals for insulin exocytosis in pancreatic beta-cells. *Cell. Mol. Life. Sci.* 59, 1803-1818
- Maechler, P., Jornot, L. and Wollheim, C.B. (1999) Hydrogen peroxide alters mitochondrial activation and insulin secretion in pancreatic beta cells. *J. Biol. Chem.* 274, 27905-27913
- McCluskey, J.T., Hamid, M., Guo-Parke, H., McClenaghan, N.H., Gomis, R. and Flatt, P.R. (2011) Development and functional characterization of insulin-releasing human pancreatic beta cell lines produced by electrofusion. *J. Biol. Chem.* 286, 21982-21992.
- Meglasson, M. D., Manning, C. D., Najafi, H., & Matschinsky, F. M. (1987). Fuel-stimulated insulin secretion by clonal hamster  $\beta$ -cell line HIT T-15. *Diabetes*, 36(4), 477-484.
- Miyazaki, J.I., Araki, K., Yamato, E., Ikegami, H., Asano, T., Shibasaki, Y. and Yamamura, K.I. (1990). Establishment of a Pancreatic  $\beta$  Cell Line That Retains Glucose-Inducible Insulin Secretion: Special Reference to Expression of Glucose Transporter Isoforms. *Endocrinology*. 127, 126-132



- Nahon, E., Israelson, A., Abu-Hamad, S. and Shoshan-Barmatz, V. (2005) Fluoxetine (Prozac) interaction with the mitochondrial voltage-dependent anion channel and protection against apoptotic cell death. *FEBS. Letts.* 579, 5105-5110
- Nakashima, K., Kanda, Y., Hirokawa, Y., Kawasaki, F. and Matsuki, M., (2009) MIN6 is not a pure beta cell line but a mixed cell line with other pancreatic endocrine hormones. *Endocrine journal.* 56, 45-53
- Ortsäter, H., Liss, P., Åkerman, K. E., & Bergsten, P. (2002). Contribution of glycolytic and mitochondrial pathways in glucose-induced changes in islet respiration and insulin secretion. *Pflügers Archiv*, 444(4), 506-512
- Pan, S.Q., Okereke, O., Rexrode, K.M., Rubin, R.R., Lucas, M., Willett, C., Manson, J.E. and Hu, F.B. (2012) Use of antidepressant medication and risk of type 2 diabetes: results from three cohorts of US adults *Diabetologia* 55, 63–72
- Reis, M., Aamo, T., Spigset, O., and Ahlner, J. (2009). Serum concentrations of antidepressant drugs in a naturalistic setting: compilation based on a large therapeutic drug monitoring database. *Therapeutic drug monitoring*, 31(1), 42-56.
- Rubin, R.R., Ma, Y., Marrero, D.G., Peyrot, M., Barrett-Connor, E.I., Kahn, S.E., Haffner, S.M., Price, D.W. and Knowler, W.C. (2008) Elevated Depression Symptoms, Antidepressant Medicine Use, and Risk of Developing Diabetes During the Diabetes Prevention Program *Diabetes. Care.* 31, 420-426
- Rustenbeck, I., Herrmann, C. and Grimmsmann, T., (1997) Energetic requirement of insulin secretion distal to calcium influx. *Diabetes* 46, 1305-1311
- Sakai, K., Matsumoto, K., Nishikawa, T., Suefuji, M., Nakamaru, K., Hirashima, Y., Kawashima, J., Shirotani, T., Ichinose, K., Brownlee, M. and Araki, E. (2003) Mitochondrial reactive oxygen species reduce insulin secretion by pancreatic beta-cells. *Biochem. Bioph. Res. Co.* 300, 216-222
- Schulz, M., Iwersen-Bergmann, S., Andresen, H. and Schmoldt, A. (2012) Therapeutic and toxic blood concentrations of nearly 1,000 drugs and other xenobiotics. *Crit. Care.* 6, 136
- Sener, A.B., Levy, J.O. and Malaisse, W.J. (1976) The stimulus-secretion coupling of glucose-induced insulin release. Does glycolysis control calcium transport in the B-cell? *Biochem. J.* 156, 521-525
- Smith, P.A., Rorsman, P. and Ashcroft, F.M. (1989) Modulation of dihydropyridine-sensitive  $Ca^{2+}$  channels by glucose metabolism in mouse pancreatic beta-cells. *Nature*, 342, 550-553.

- Smith, P.A., Sellers, L.A. and Humphrey, P.P. (2001) Somatostatin activates two types of inwardly rectifying K<sup>+</sup> channels in MIN-6 cells. *J. Physiol.* 532,127-142.
- Souza, M.E., Polizello, A.C., Uyemura, S.A., Castro-Silva, O. and Curti, C. (1994) Effect of fluoxetine on rat liver mitochondria. *Biochem. Pharmacol.* 48, 535-54
- Sugimoto, Y., Inoue, K. and Yamada, J. (2003) The tricyclic antidepressant clomipramine increases plasma glucose levels of mice. *J. Pharmacol. Sci.* 93, 74-79
- Uguz, F., Sahingoz, M., Gungor, B., Aksoy, F. and Askin, R. (2015) Weight gain and associated factors in patients using newer antidepressant drugs. *Gen. Hosp. Psychiat.* 37, 46-48
- Weinbach, E.C., Costa, J.L., Nelson, B.D., Claggett, C.E., Hundal, T., Bradley, D. and Morris, S.J. (1986) Effects of tricyclic antidepressant drugs on energy-linked reactions in mitochondria. *Biochem. Pharmacol.* 35, 1445-1451
- Winek, C.L., Wahba, W.W., Winek, C.L. Jr and Balzer, T.W. (2001) Drug and chemical blood-level data 2001. *Forensic. Sci. Int.* 122, 107-123.
- Woynillowicz, A.K., Raha, S., Nicholson, C.J. and Holloway, A.C. (2012) The effect of smoking cessation pharmacotherapies on pancreatic beta cell function. *YTAAP* 265, 122-127.
- Xia, Z., Lundgren, B., Bergstrand, A., De Pierre, J.W. and Nassberger, L. (1999) Changes in the generation of reactive oxygen species and in mitochondrial membrane potential during apoptosis induced by the antidepressants imipramine, clomipramine, and citalopram and the effects on these changes by Bcl-2 and Bcl-X(L). *Biochem. Pharmacol.* 57, 1199–1208.
- Yamada, J., Sugimoto, Y. and Inoue, K. (1999) Selective serotonin reuptake inhibitors fluoxetine and fluvoxamine induce hyperglycemia by different mechanisms. *Euro. J. Pharmacol.* 382, 211-215

## Figure Captions

**Fig. 1 Antidepressants inhibit MTT reduction.** **A)** Absorbance of MTT reduction measured (arbitrary units, A.U.) in a murine pancreatic  $\beta$  cell-line (MIN6) under control conditions as a function of time. Each point is a triplicate average from a separate experiment ( $n = 9$ ). **B-D)** Concentration-effect relationships for the effect of paroxetine (**B**), fluoxetine (**C**) and clomipramine (**D**) on the reduction of MTT measured after 4 different times of incubation as indicated:  $\bullet$ , 4 hrs;  $\blacksquare$ , 24 hrs;  $\blacktriangle$ , 48 hrs;  $\blacktriangledown$ , 72 hrs. Data are mean  $\pm$  SD as a percentage of values measured under control conditions ( $n = 9$  in all cases). Solid lines are fits of equation 1 to the data with the parameter values given in **E**) and **F**). **E-F)** Time courses of  $IC_{50}$  and pedestal respectively for the inhibition of MTT reduction by the drugs indicated:  $\bullet$ , PAR, paroxetine;  $\blacksquare$ , FLX, fluoxetine;  $\blacktriangle$ , CLM, clomipramine. For **E**) data is given as mean  $\pm$  95% C.I., for **F**) data is mean  $\pm$  SEM ( $n = 9$ ). Solid line in **E** is a fit of equation 2 to the FLX data with parameter values given in the text. **G)** Time course for inhibition of MTT reduction by 100 nM AD taken from **B**, **C** and **D**. Data mean  $\pm$  SD ( $n = 9$ ). The effect of all three ADs are positively correlated with time (Pearson,  $r > 0.98$  and  $P < 0.05$  for all cases). **H)** Effect of ADs in the absence (open bars) and presence (filled bars) of 10  $\mu$ M GSH. Cells were incubated for 24 hours in 55  $\mu$ M paroxetine (PAR), 29  $\mu$ M fluoxetine (FLX) or 44  $\mu$ M clomipramine (CLM); concentrations that inhibit MTT reduction by  $\sim 50\%$  over this time period. Data mean  $\pm$  SD ( $n = 9$ ). Statistical significance determined by Paired t-test.

**Fig. 2 Antidepressants inhibit ATP production and mitochondrial Complex activity.** **a-d)** Comparison of the concentration-effect relationships for three ADs on MTT and ATP levels in MIN6 cells after 24 hours of incubation. Effect of paroxetine (**A**), fluoxetine (**B**) and clomipramine (**C**). Data are the mean  $\pm$  SD as a percentage of control values ( $n = 9$  in all cases). Solid lines are fits of equation 1 to the data with the  $IC_{50}$ s given in **D**). **D)** Comparison of the  $IC_{50}$ 's for the inhibition of MTT reduction ( $\bullet$ ) and ATP production ( $\blacksquare$ ) by the drugs indicated: PAR, paroxetine; FLX, fluoxetine; CLM, clomipramine. Data given as mean  $\pm$  95% C.I. Data is from 9 experiments in each case. **E-F)** Comparison between the effects of 55  $\mu$ M paroxetine (PAR), 29  $\mu$ M fluoxetine (FLX) and 44  $\mu$ M clomipramine (CLM) on the activity of mitochondrial Complex I activity (**E**) and Complex III activity (**F**) after 24 hr incubation. Data

shown as mean  $\pm$  SD (n = 3). ). Statistical significance determined by One sample t-test with a theoretical mean of 100%.

**Fig. 3 Antidepressants inhibit insulin secretion increase lactate output and promote reactive species generation.** Cells were incubated for 24 hours in 55  $\mu$ M paroxetine (PAR), 30  $\mu$ M fluoxetine (FLX) or 45  $\mu$ M clomipramine (CLM). Data are shown either as raw values or as a percentage of values measured under control conditions: for lactate production (**A & C** respectively) and generation of reactive oxygen species (ROS) (**B & D** respectively). **E**) Insulin secretion stimulated in response to 25 mM glucose for a 15 minutes period post AD treatment. **F**) Cell count after 24 hr incubation at the concentrations of AD given above. Results are expressed as mean  $\pm$  SD (n = 3 for each situation). **G**) Caspase activity after 24 hr incubation at the concentrations of AD given above. Results are expressed as mean  $\pm$  SD (n = 3-9 for each situation). Open bars, caspase 3; light bars, caspase 8, dark bars, caspase 9. Statistical significance for A, B, E and F was determined by One sample t-test with a theoretical mean of 100%. Statistical significance for C, D and G was determined by One way ANOVA with Dunnett's multiple comparisons test relative to control.

**Fig. 4. Fluoxetine inhibits oxygen consumption.** **A)** Representative records of oxygen concentration for three different suspensions of MIN6 cells showing stimulation of oxygen consumption (respiration) by 10 mM glucose and the subsequent inhibition by 10, 30 and 100  $\mu$ M fluoxetine. **B)** Fluoxetine concentration-response relationship for OCR inhibition as a percentage of that measured in 10 mM glucose for MIN6 (●) and human 1.1B4 (○) cell lines. Data are means  $\pm$  SD (n= 6 - 29). See text for details of fitted lines. Statistical significance is relative to vehicle control determined via Kruskal-Wallis for MIN6. **C)** Percentage change in OCR relative to that measured in the absence of exogenous substrate (basal) under the conditions indicated: Glu, 10 mM glucose and then 100  $\mu$ M fluoxetine, FLX; Glu, 10 mM glucose, then 100 nM FCCP followed by 100  $\mu$ M fluoxetine, FFLX. Data are means  $\pm$  SD (n= 10 – 17 Statistical significance determined by 1-way ANOVA with Sidak's multiple comparison test. **D)** OCR of 6 different pancreatic islet preparations measured under the conditions indicated: Bas, basal in the absence of exogenous substrate; Glu, in 20 mM glucose; FLX, 20 mM glucose and 100  $\mu$ M

fluoxetine. Statistical significance determined by 1-way ANOVA with Sidak's multiple comparison test.

**Fig. 5. Substrate independent effects of fluoxetine on respiration.** **A)** Oxygen consumption rate (OCR) stimulated by methyl-O-glucose (MOG,  $n = 42$ ), D-glucose (GLU,  $n = 71$ ), D-glyceraldehyde (GLY,  $n = 34$ ), methylpyruvate (MP,  $n = 30$ ) and  $\alpha$ -ketoisocaproate (KIC,  $n = 33$ ), all at 10 mM, and by tetramethyl-p-phenylenediamine/ascorbate (ASB;  $n = 45$ ). Data are box and whisker (Tukey). Statistical significance is relative to MOG determined via Kruskal-Wallis with Dunn's multiple comparison test. **B)** Percentage inhibition of OCR by 30  $\mu$ M fluoxetine in the presence of the same substrates as in **A** ( $n = 8-25$ ). Statistical significance is relative to respective water controls via Mann-Whitney. Data are box and whisker (Tukey). **C)** Spearman  $r$  values and associated probabilities for the correlation between magnitude of inhibition produced by 30  $\mu$ M fluoxetine and basal OCR (open columns) or OCR stimulated by the substrates indicated (closed columns): MOG (3-O-methylglucose,  $n = 8$ ), GLU (glucose,  $n = 25$ ), GLY (DL-glyceraldehyde,  $n = 10$ ); MP (methyl-pyruvate,  $n = 8$ ), KIC ( $\alpha$ -ketoisocaproic acid,  $n = 10$ ) all at 10 mM and ASB (TMPD/ascorbate,  $n = 10$ ). **D)** Correlation between the decline in OCR produced by 30  $\mu$ M fluoxetine (FLX) and basal OCR ( $n = 24$ ). **E)** Glucose concentration-response relationships for OCR relative to basal in the absence (●) and presence (○) of 100  $\mu$ M fluoxetine, ( $n = 5-8$ ). Data are means  $\pm$  SD. Note the similar difference between the two sets of data for each glucose concentration. **F)** Glucose concentration-response relationships for the % inhibition of OCR by 100  $\mu$ M fluoxetine. Data are means  $\pm$  SD and are calculated from that shown **E**.

**Fig. 6. Acute fluoxetine stimulates lactate production.** Simultaneously measured changes in oxygen consumption rate ( $\Delta$ OCR) and lactate production ( $\Delta$ Lactate) compared to those measured in the absence of exogenous substrate (basal). **A-B)** Effect of 10 mM glucose (Glu), and then 30  $\mu$ M fluoxetine (FLX) in the continued presence of the sugar on OCR (**A**) and lactate output (**B**) from the same 5 sets of experiments (matched by symbol). **C-D)** Effects of 10 mM glucose (Glu), and 1  $\mu$ M rotenone (Rot) in the continued presence of the sugar on OCR (**C**) and lactate output (**D**) from the same 5 sets of experiments (matched by symbol). Note that rotenone

inhibits OCR beyond that measured in basal to give a negative value. **E-F)** Comparison of the effects of 30  $\mu$ M fluoxetine in the presence of 10 mM glucose (Glu) on OCR (**E**) and lactate output (**F**) for MIN6 (MIN6F; n = 5) and 1.1B4 (11B4; n = 5). Statistical significance is via Mann-Whitney.

**Fig. 7. Rh123 fluorescence as a measure of the mitochondrial membrane potential,  $\Delta\Psi_{mit}$ .** Effects of 10 mM glucose and drugs as indicated on  $\Delta\Psi_{mit}$ , in MIN6 cells. **A-D)**  $\Delta\Psi_{mit}$  is represented by the change in Rh-123 fluorescence relative to that measured in the absence of the sugar (100%). Compounds were applied for the duration of the bars. Records are representative of at least 3 different experiments for each condition and are formed from the average of at least 7 ROIs. **A)** Effects of 10 mM glucose, 2.5  $\mu$ g ml<sup>-1</sup> oligomycin (Olig), 1  $\mu$ M antimycin A (AntA) and 1  $\mu$ M FCCP (FC). **B)** The effects of 10 mM glucose, 30  $\mu$ M fluoxetine (FLX) followed by 1  $\mu$ M FCCP (FC). **C)** Effects of 10 mM glucose, 1  $\mu$ M rotenone (Rot) 30  $\mu$ M fluoxetine (FLX) and 1  $\mu$ M FCCP (FC). **D)** The effect of water then 1  $\mu$ M FCCP (FC) in the presence of 10 mM glucose. **E)** Concentration-response relationship for the initial rate of Rh123 fluorescence increase ( $\Delta$ Rh123) produced by fluoxetine (●). Data are the means  $\pm$ SD (n = 3-9). Statistical significance is via ANOVA with Dunnett's post comparison test relative to water control. **F)** Box and whisker (Tukey) comparison of Rh123 fluorescence relative to basal (100%); GLU, effect of glucose (n = 184); FLX, plus 30  $\mu$ M fluoxetine (n = 156); H2O, water control (n = 28). Data is from at least 5 independent preparations in each case, where n is the total number of ROI measured for each condition. Statistical significance is via Kruskal-Wallis with Dunn's multiple comparison test.

**Fig. 8. MitoSOX fluorescence as a measure of mitochondrial superoxide generation. A-C)** Representative images of MIN6 cells in DMSO (**A**), 30  $\mu$ M fluoxetine (**B**) and 1  $\mu$ M antimycin (**C**) all for 1 hr from the same experimental run. Red fluorescence demonstrates the detection of the superoxide anion by the MitoSOX dye. Scale bar 30  $\mu$ m, all images at 50% brightness. **D)** Amount of superoxide generated, measured in arbitrary fluorescence units under the conditions indicated: Ctrl, basal conditions (n = 8); DMSO, vehicle control for fluoxetine and antimycin (n = 5); FLX, 30  $\mu$ M fluoxetine (n = 7); ANTA, 1  $\mu$ M antimycin (n = 9) Data are the means  $\pm$  SD .

**Fig. 9. Cell-attached study of  $K_{ATP}$  channel activity** **A)** Representative records of  $K_{ATP}$  channel activity measured from the same MIN6 cell under the successive conditions indicated. Dotted line is the zero-current level, openings are downward. **B)** Box and whisker (Tukey) comparison of  $K_{ATP}$  channel activity (NPo) normalised to that measured in zero glucose; Ctrl, perfusion control (n = 10), Glucose, 10 mM Glucose (n = 46). **C)** Box and whisker (Tukey) comparison of  $K_{ATP}$  channel activity reactivated, as a % of that blocked by 10 mM glucose, with the treatments indicated; H<sub>2</sub>O, water vehicle control (n = 8); 1F, 1  $\mu$ M fluoxetine (n = 7); 3F, 3  $\mu$ M fluoxetine (n = 5); 10F, 10  $\mu$ M fluoxetine (n = 5); 30F, 30  $\mu$ M fluoxetine (n = 8); 100F, 100  $\mu$ M fluoxetine (n = 5); Rot, 1  $\mu$ M rotenone (n = 6); FCCP, 100 nM FCCP (n = 16); Tol, 100 nM FCCP + 20  $\mu$ M tolbutamide (n = 9) Ant, 1  $\mu$ M antimycin (n = 4).

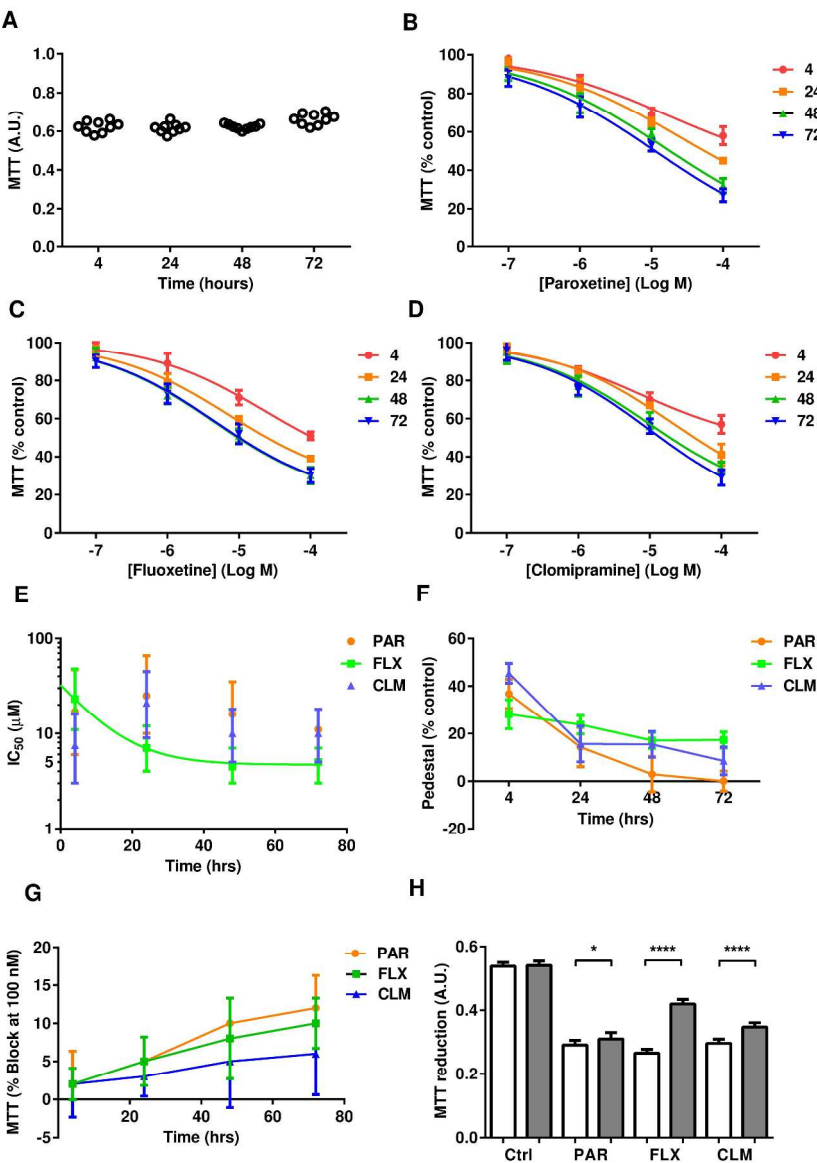


Fig. 1 Antidepressants inhibit MTT reduction. A) Absorbance of MTT reduction measured (arbitrary units, A.U.) in a murine pancreatic  $\beta$  cell-line (MIN6) under control conditions as a function of time. Each point is a triplicate average from a separate experiment ( $n = 9$ ). B-D) Concentration-effect relationships for the effect of paroxetine (B), fluoxetine (C) and clomipramine (D) on the reduction of MTT measured after 4 different times of incubation as indicated:  $\bullet$ , 4 hrs;  $\blacksquare$ , 24 hrs;  $\triangle$ , 48 hrs;  $\nabla$ , 72 hrs. Data are mean  $\pm$  SD as a percentage of values measured under control conditions ( $n = 9$  in all cases). Solid lines are fits of equation 1 to the data with the parameter values given in E) and F). E-F) Time courses of IC50 and pedestal respectively for the inhibition of MTT reduction by the drugs indicated:  $\bullet$ , PAR, paroxetine;  $\blacksquare$ , FLX, fluoxetine;  $\triangle$ , CLM, clomipramine. For E) data is given as mean  $\pm$  95% C.I., for F) data is mean  $\pm$  SEM ( $n = 9$ ). Solid line in E is a fit of equation 2 to the FLX data with parameter values given in the text. G) Time course for inhibition of MTT reduction by 100 nM AD taken from B, C and D. Data mean  $\pm$  SD ( $n = 9$ ). The effect of all three ADs are positively correlated with time (Pearson,  $r > 0.98$  and  $P < 0.05$  for all cases). H) Effect of ADs in the absence (open bars) and presence (filled bars) of 10  $\mu$ M GSH. Cells were incubated for



24 hours in 55  $\mu$ M paroxetine (PAR), 29  $\mu$ M fluoxetine (FLX) or 44  $\mu$ M clomipramine (CLM); concentrations that inhibit MTT reduction by  $\sim$  50% over this time period. Data mean  $\pm$  SD (n = 9). Statistical significance determined by Paired t-test.

293x404mm (300 x 300 DPI)

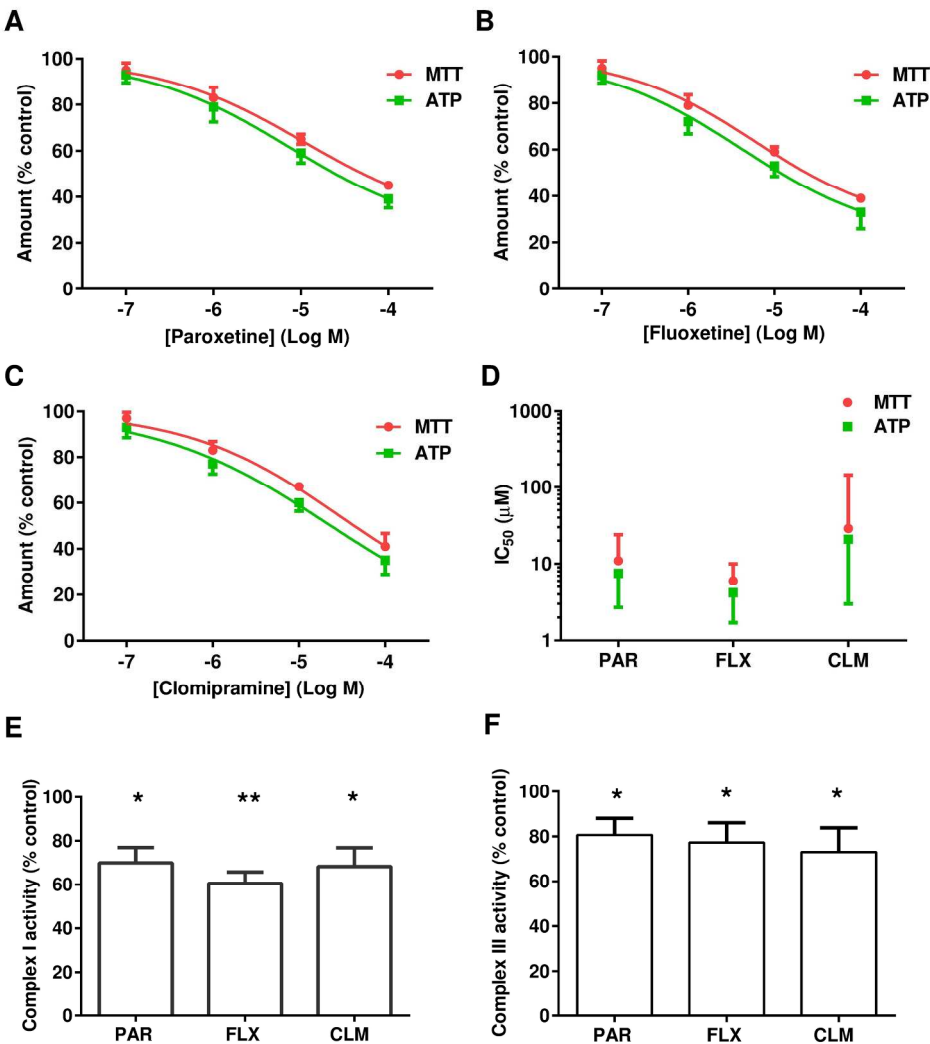


Fig. 2 Antidepressants inhibit ATP production and mitochondrial Complex activity. a-d) Comparison of the concentration-effect relationships for three ADs on MTT and ATP levels in MIN6 cells after 24 hours of incubation. Effect of paroxetine (A), fluoxetine (B) and clomipramine (C). Data are the mean  $\pm$  SD as a percentage of control values ( $n = 9$  in all cases). Solid lines are fits of equation 1 to the data with the IC<sub>50</sub>s given in D). D) Comparison of the IC<sub>50</sub>'s for the inhibition of MTT reduction (●) and ATP production (■) by the drugs indicated: PAR, paroxetine; FLX, fluoxetine; CLM, clomipramine. Data given as mean  $\pm$  95% C.I. Data is from 9 experiments in each case. E-F) Comparison between the effects of 55  $\mu$ M paroxetine (PAR), 29  $\mu$ M fluoxetine (FLX) and 44  $\mu$ M clomipramine (CLM) on the activity of mitochondrial Complex I activity (E) and Complex III activity (F) after 24 hr incubation. Data shown as mean  $\pm$  SD ( $n = 3$ ). Statistical significance determined by One sample t-test with a theoretical mean of 100%.

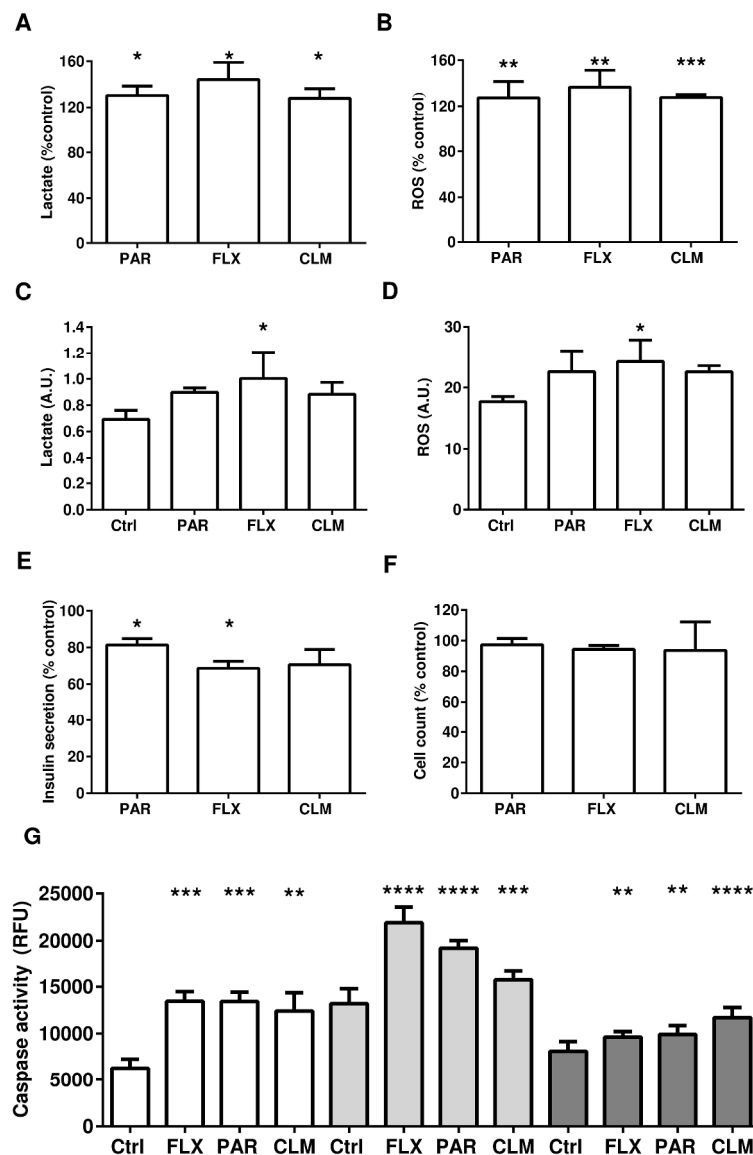


Fig. 3 Antidepressants inhibit insulin secretion increase lactate output and promote reactive species generation. Cells were incubated for 24 hours in 55  $\mu$ M paroxetine (PAR), 30  $\mu$ M fluoxetine (FLX) or 45  $\mu$ M clomipramine (CLM). Data are shown either as raw values or as a percentage of values measured under control conditions: for lactate production (A & C respectively) and generation of reactive oxygen species (ROS) (B & D respectively). E) Insulin secretion stimulated in response to 25 mM glucose for a 15 minutes period post AD treatment. F) Cell count after 24 hr incubation at the concentrations of AD given above. Results are expressed as mean  $\pm$  SD ( $n = 3$  for each situation). G) Caspase activity after 24 hr incubation at the concentrations of AD given above. Results are expressed as mean  $\pm$  SD ( $n = 3-9$  for each situation). Open bars, caspase 3; light bars, caspase 8, dark bars, caspase 9. Statistical significance for A, B, E and F was determined by One sample t-test with a theoretical mean of 100%. Statistical significance for C, D and G was determined by One way ANOVA with Dunnett's multiple comparisons test relative to control.

1  
2  
3  
4  
5  
6  
7  
8  
9  
10  
11  
12  
13  
14  
15  
16  
17  
18  
19  
20  
21  
22  
23  
24  
25  
26  
27  
28  
29  
30  
31  
32  
33  
34  
35  
36  
37  
38  
39  
40  
41  
42  
43  
44  
45  
46  
47  
48  
49  
50  
51  
52  
53  
54  
55  
56  
57  
58  
59  
60

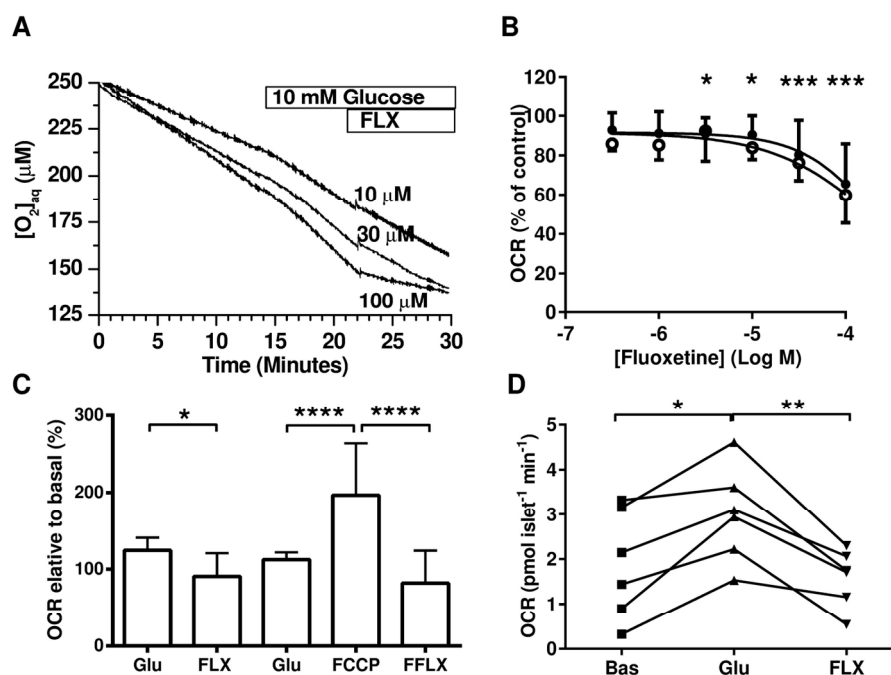


Fig. 4. Fluoxetine inhibits oxygen consumption. A) Representative records of oxygen concentration for three different suspensions of MIN6 cells showing stimulation of oxygen consumption (respiration) by 10 mM glucose and the subsequent inhibition by 10, 30 and 100  $\mu$ M fluoxetine. B) Fluoxetine concentration-response relationship for OCR inhibition as a percentage of that measured in 10 mM glucose for MIN6 ( $\bullet$ ) and human 1.1B4 ( $\circ$ ) cell lines. Data are means  $\pm$  SD ( $n = 6 - 29$ ). See text for details of fitted lines. Statistical significance is relative to vehicle control determined via Kruskal-Wallis for MIN6. C) Percentage change in OCR relative to that measured in the absence of exogenous substrate (basal) under the conditions indicated: Glu, 10 mM glucose and then 100  $\mu$ M fluoxetine, FLX; Glu, 10 mM glucose, then 100 nM FCCP followed by 100  $\mu$ M fluoxetine, FFLX. Data are means  $\pm$  SD ( $n = 10 - 17$ ). Statistical significance determined by 1-way ANOVA with Sidak's multiple comparison test. D) OCR of 6 different pancreatic islet preparations measured under the conditions indicated: Bas, basal in the absence of exogenous substrate; Glu, in 20 mM glucose; FLX, 20 mM glucose and 100  $\mu$ M fluoxetine. Statistical significance determined by 1-way ANOVA with Sidak's multiple comparison test.

151x109mm (300 x 300 DPI)

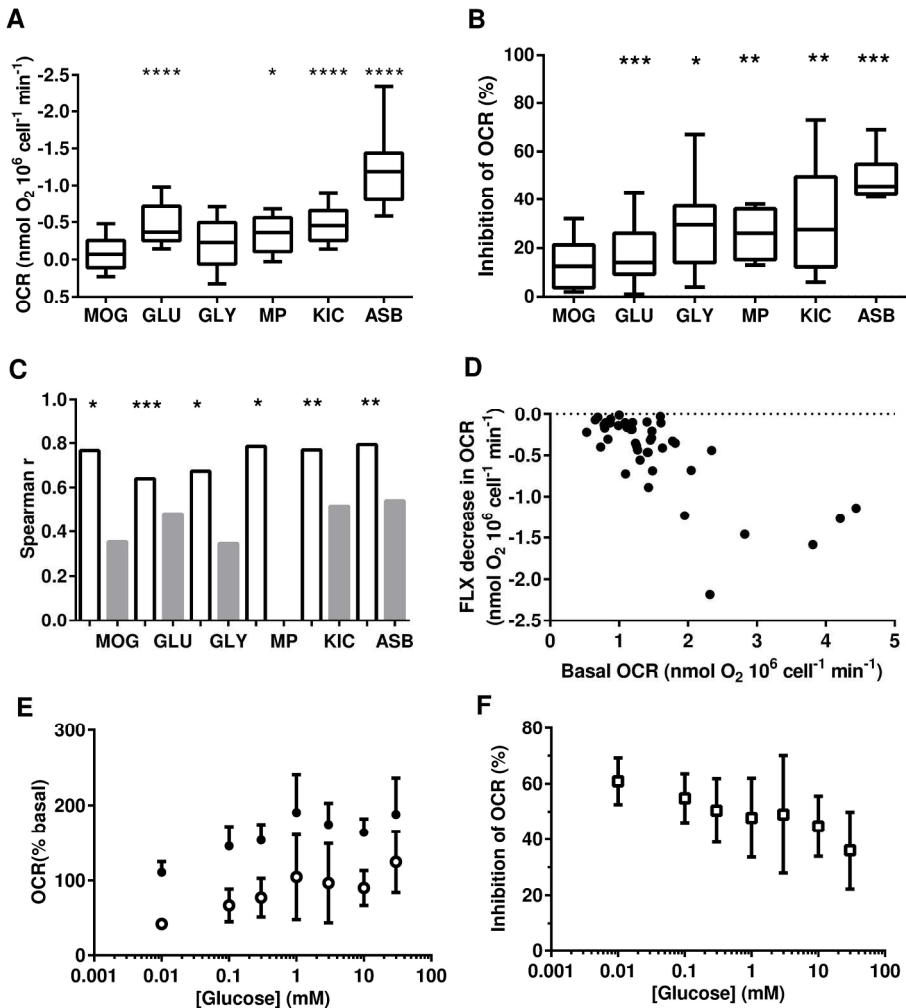


Fig. 5. Substrate independent effects of fluoxetine on respiration. A) Oxygen consumption rate (OCR) stimulated by methyl-O-glucose (MOG,  $n = 42$ ), D-glucose (GLU,  $n = 71$ ), D-glyceraldehyde (GLY,  $n = 34$ ), methylpyruvate (MP,  $n = 30$ ) and  $\alpha$ -ketoisocaproate (KIC,  $n = 33$ ), all at 10 mM, and by tetramethyl-p-phenylenediamine/ascorbate (ASB;  $n = 45$ ). Data are box and whisker (Tukey). Statistical significance is relative to MOG determined via Kruskal-Wallis with Dunn's multiple comparison test. B) Percentage inhibition of OCR by 30  $\mu\text{M}$  fluoxetine in the presence of the same substrates as in A ( $n = 8$ -25). Statistical significance is relative to respective water controls via Mann-Whitney. Data are box and whisker (Tukey). C) Spearman  $r$  values and associated probabilities for the correlation between magnitude of inhibition produced by 30  $\mu\text{M}$  fluoxetine and basal OCR (open columns) or OCR stimulated by the substrates indicated (closed columns): MOG (3-O-methylglucose,  $n = 8$ ), GLU (glucose,  $n = 25$ ), GLY (DL-glyceraldehyde,  $n = 10$ ); MP (methyl-pyruvate,  $n = 8$ ), KIC ( $\alpha$ -ketoisocaproic acid,  $n = 10$ ) all at 10 mM and ASB (TMPD/ascorbate,  $n = 10$ ). D) Correlation between the decline in OCR produced by 30  $\mu\text{M}$  fluoxetine (FLX) and basal OCR ( $n = 24$ ). E) Glucose concentration-response relationships for OCR relative to basal in the absence (●) and presence (○) of 100  $\mu\text{M}$  fluoxetine, ( $n = 5$ -8). Data are means  $\pm$  SD. Note the similar difference between the two sets of data for each glucose concentration. F) Glucose concentration-response relationships for the % inhibition of OCR by 100  $\mu\text{M}$  fluoxetine. Data are means  $\pm$  SD and are calculated from that shown E.

226x238mm (300 x 300 DPI)

1  
2  
3  
4  
5  
6  
7  
8  
9  
10  
11  
12  
13  
14  
15  
16  
17  
18  
19  
20  
21  
22  
23  
24  
25  
26  
27  
28  
29  
30  
31  
32  
33  
34  
35  
36  
37  
38  
39  
40  
41  
42  
43  
44  
45  
46  
47  
48  
49  
50  
51  
52  
53  
54  
55  
56  
57  
58  
59  
60

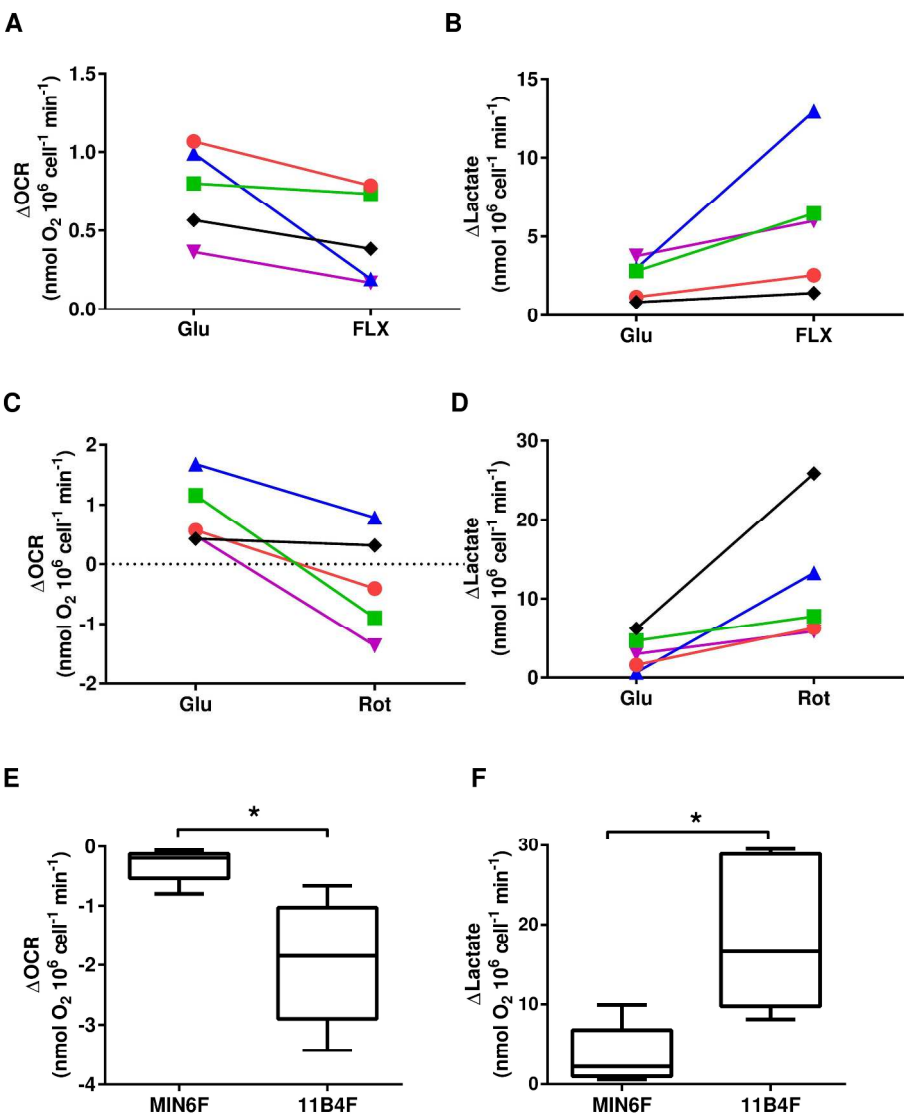


Fig. 6. Acute fluoxetine stimulates lactate production. Simultaneously measured changes in oxygen consumption rate ( $\Delta OCR$ ) and lactate production ( $\Delta Lactate$ ) compared to those measured in the absence of exogenous substrate (basal). A-B Effect of 10 mM glucose (Glu), and then 30  $\mu M$  fluoxetine (FLX) in the continued presence of the sugar on OCR (A) and lactate output (B) from the same 5 sets of experiments (matched by symbol). C-D Effects of 10 mM glucose (Glu), and 1  $\mu M$  rotenone (Rot) in the continued presence of the sugar on OCR (C) and lactate output (D) from the same 5 sets of experiments (matched by symbol). Note that rotenone inhibits OCR beyond that measured in basal to give a negative value. E-F Comparison of the effects of 30  $\mu M$  fluoxetine in the presence of 10 mM glucose (Glu) on OCR (E) and lactate output (F) for MIN6 (MIN6F; n = 5) and 1.1B4 (11B4; n = 5). Statistical significance is via Mann-Whitney.



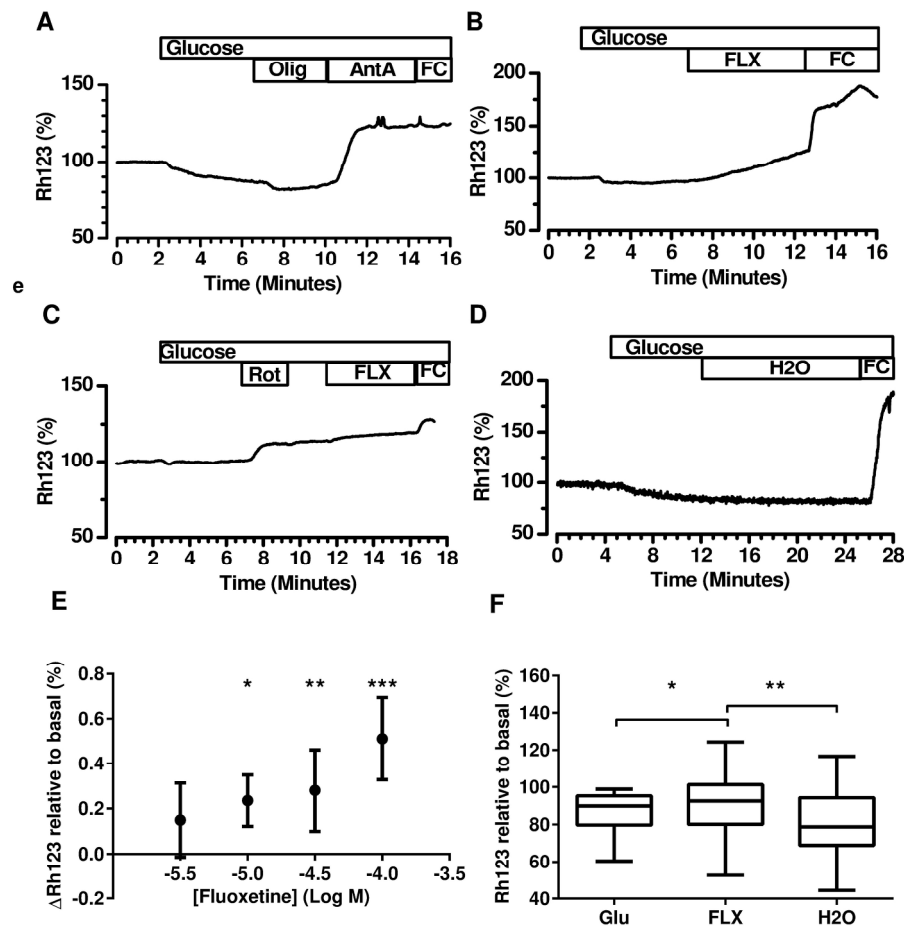


Fig. 7. Rh123 fluorescence as a measure of the mitochondrial membrane potential,  $\Delta\Psi_{mit}$ . Effects of 10 mM glucose and drugs as indicated on  $\Delta\Psi_{mit}$ , in MIN6 cells. A-D)  $\Delta\Psi_{mit}$  is represented by the change in Rh-123 fluorescence relative to that measured in the absence of the sugar (100%). Compounds were applied for the duration of the bars. Records are representative of at least 3 different experiments for each condition and are formed from the average of at least 7 ROIs. A) Effects of 10 mM glucose, 2.5  $\mu$ g ml<sup>-1</sup> oligomycin (Olig), 1  $\mu$ M antimycin A (AntA) and 1  $\mu$ M FCCP (FC). B) The effects of 10 mM glucose, 30  $\mu$ M fluoxetine (FLX) followed by 1  $\mu$ M FCCP (FC). C) Effects of 10 mM glucose, 1  $\mu$ M rotenone (Rot) 30  $\mu$ M fluoxetine (FLX) and 1  $\mu$ M FCCP (FC). D) The effect of water then 1  $\mu$ M FCCP (FC) in the presence of 10 mM glucose. E) Concentration-response relationship for the initial rate of Rh123 fluorescence increase ( $\Delta$ Rh123) produced by fluoxetine ( $\bullet$ ). Data are the means  $\pm$  SD (n = 3-9). Statistical significance is via ANOVA with Dunnett's post comparison test relative to water control. F) Box and whisker (Tukey) comparison of Rh123 fluorescence relative to basal (100%); GLU, effect of glucose (n = 184); FLX, plus 30  $\mu$ M fluoxetine (n = 156); H2O, water control (n = 28). Data is from at least 5 independent preparations in each case, where n is the total number of ROI measured for each condition. Statistical significance is via Kruskal-Wallis with Dunn's multiple comparison test.

220x220mm (300 x 300 DPI)

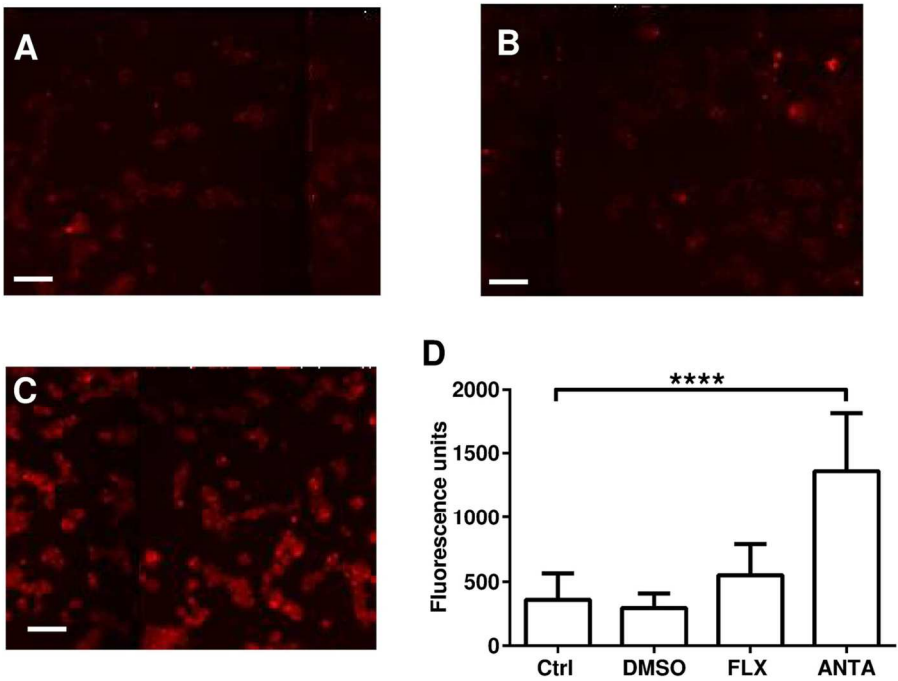


Fig. 8. MitoSOX fluorescence as a measure of mitochondrial superoxide generation. A-C) Representative images of MIN6 cells in DMSO (A), 30  $\mu$ M fluoxetine (B) and 1  $\mu$ M antimycin (C) all for 1 hr from the same experimental run. Red fluorescence demonstrates the detection of the superoxide anion by the MitoSOX dye. Scale bar 30  $\mu$ m, all images at 50% brightness. D) Amount of superoxide generated, measured in arbitrary fluorescence units under the conditions indicated: Ctrl, basal conditions (n = 8); DMSO, vehicle control for fluoxetine and antimycin (n = 5); FLX, 30  $\mu$ M fluoxetine (n = 7); ANTA, 1  $\mu$ M antimycin (n = 9) Data are the means  $\pm$  SD .

120x89mm (300 x 300 DPI)

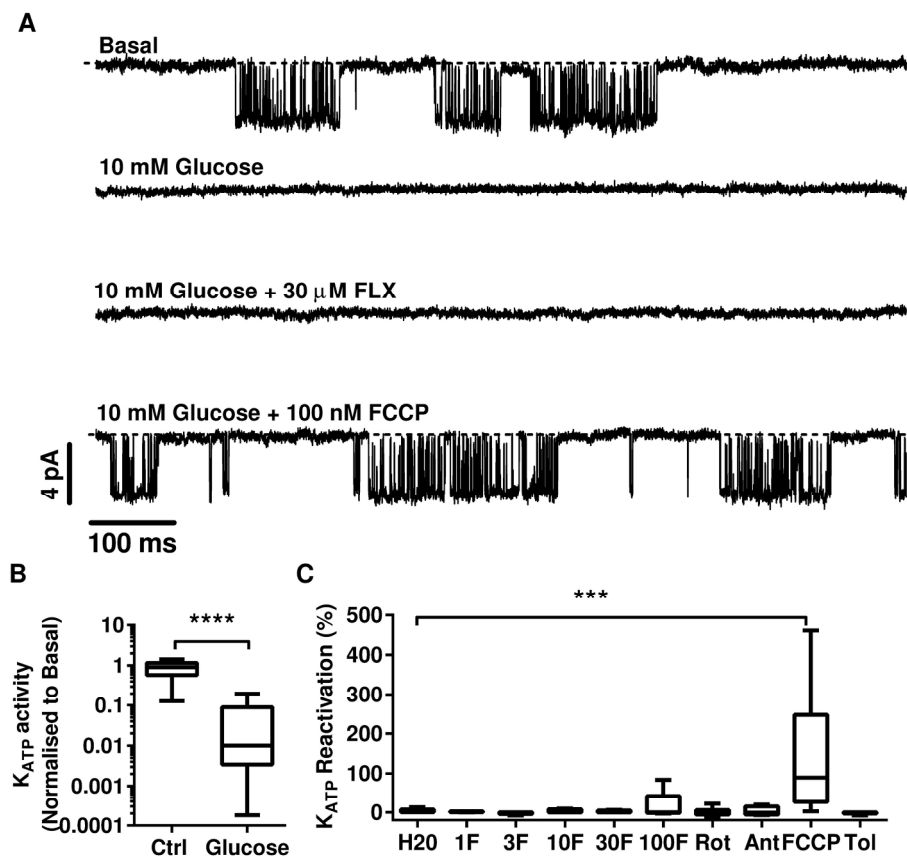


Fig. 9. Cell-attached study of KATP channel activity A) Representative records of KATP channel activity measured from the same MIN6 cell under the successive conditions indicated. Dotted line is the zero-current level, openings are downward. B) Box and whisker (Tukey) comparison of KATP channel activity (NPo) normalised to that measured in zero glucose; Ctrl, perfusion control (n = 10), Glucose, 10 mM Glucose (n = 46). C) Box and whisker (Tukey) comparison of KATP channel activity reactivated, as a % of that blocked by 10 mM glucose, with the treatments indicated; H2O, water vehicle control (n = 8); 1F, 1  $\mu$ M fluoxetine (n = 7); 3F, 3  $\mu$ M fluoxetine (n = 5); 10F, 10  $\mu$ M fluoxetine (n = 5); 30F, 30  $\mu$ M fluoxetine (n = 8); 100F, 100  $\mu$ M fluoxetine (n = 5); Rot, 1  $\mu$ M rotenone (n = 6); FCCP, 100 nM FCCP (n = 16); Tol, 100 nM FCCP + 20  $\mu$ M tolbutamide (n = 9); Ant, 1  $\mu$ M antimycin (n = 4).

200x181mm (300 x 300 DPI)